J. Micropalaeontology, 45, 335–357, 2026
https://doi.org/10.5194/jm-45-335-2026

Journal of Micropalaeontology
Open Access

Palynofacies and lacustrine sequence stratigraphy: a case example from the Jurassic Cañadón Asfalto Formation, Cañadón Asfalto Basin, Extra-Andean Patagonia, Argentina

Daniela Elizabeth Olivera[1], Carlos Zavala[1], Mirta Elena Quattrocchio[2], María Eugenia Soreda[3], Roberto Scasso[4], and Renchao Yang[1,5]

[1]College of Earth Science and Engineering, Shandong University of Science and Technology, No. 579 Qianwangang Road, Qingdao, Shandong Province, 266590, China
[2]Departamento de Geología, Universidad Nacional del Sur (UNS) – Consejo Nacional de Investigaciones Científicas y Técnicas (CONICET), Avenida Alem 1253, B8000ICN Bahía Blanca, Buenos Aires, Argentina
[3]Departamento de Ciencias Geológicas, Facultad de Ciencias Exactas y Naturales, Universidad de Buenos Aires, Ciudad Universitaria Pabellón II, Intendente Güiraldes 2160, C1428EHA Ciudad Autónoma de Buenos Aires, Argentina
[4]Instituto de Geociencias Básicas, Aplicadas y Ambientales de Buenos Aires, Dpto. de Ciencias Geológicas, Facultad de Ciencias Exactas y Naturales, Universidad de Buenos Aires – CONICET, Intendente Güiraldes 2160, Pabellón II, Ciudad Universitaria, 1428 Buenos Aires, Argentina
[5]Laboratory for Marine Mineral Resources, Qingdao Marine Science and Technology Center, Qingdao, 266237, China

Correspondence: Carlos Zavala (skd995108@sdust.edu.cn)

Received: 11 January 2026 – Revised: 17 April 2026 – Accepted: 28 April 2026 – Published: 13 May 2026

Abstract. This study presents a detailed palynofacies analysis integrated with lacustrine sequence stratigraphy to evaluate the role of climate-driven hydrological balance on basin infill and its impact on the organic matter accumulation in the Jurassic Cañadón Asfalto Formation, Cerro Cóndor depocentre, Extra-Andean Patagonia, Argentina. It provides valuable insights into the changes in the nature and taphonomic history of the organic matter throughout the different stages of a lacustrine system's evolution based on the analysis of 51 outcrop samples from the Cañadón Lahuincó "A" section. Two depositional sequences are recognised. Sequence I documents the evolution from underfilled to balanced-fill/overfilled lake stages. Underfilled conditions are characterised by extreme lake-level variability, while the transition to balanced-fill/overfilled conditions is marked by stacked coarsening-upward successions. Sequence II is bounded by an abrupt accommodation increase and initially records renewed underfilled conditions, followed by the establishment of a fully overfilled lake stage characterised by persistent progradational stacking patterns. The most conspicuous feature of the Cañadón Asfalto Formation's organic matter is the overall dominance of land-derived fraction. The variations between the allochthonous and autochthonous (algae and algal-derived amorphous organic matter) material suggests variable climatic conditions, with the alternation of wetter and drier periods at least during the Sequence I and part of the Sequence II. Four palynofacies types (PT-A to PT-D) were defined recording variations in depositional energy, redox conditions, and sediment–water balance. PT-A and PT-D indicate wetter periods, while PT-B indicates relatively drier intervals. PT-C shows the changes between these two opposite situations. The underfilled stage is characterised by the dominance of reworked terrestrial phytoclasts (indicating high-energy inflow events) and poor sporomorph preservation. Conversely, the balanced-fill stage shows sporomorph-rich palynofacies. In both lake stages, blooms of well-preserved strong fluorescence *Botryococcus* colonies (chlorophytic algae) are registered during drier periods. The overfilled conditions are characterised by the lack of palynomorphs. Kerogen

varies from Type III (PT-A) to mixed Type I/III in algae-rich intervals (PT-B, PTC), confirming hydrological balance as the control on organic matter preservation.

1 Introduction

Lakes are highly dynamic systems and cannot be treated as merely small oceans (Bohacs et al., 2000). In contrast to marine basins, in lacustrine basins the lake level can dramatically fluctuate, driven by long-term dry–wet climatic cycles, which can effectively control water salinity, primary productivity, and basin accommodation (Zavala et al., 2024). This is especially evident in closed lakes, where the supply of sediment and organic matter is accompanied by the introduction of a huge volume of water, resulting in a lake transgression. As an example, most world rivers have a suspended sediment concentration of less than $1\,g\,L^{-1}$ (Mulder and Syvitski, 1995). Roughly speaking, this means that a basin commonly receives 1000 times more water than sediments. As a consequence, allocyclic processes such as climate and tectonics become key elements that control the accumulation and preservation of clastic and organic materials in lacustrine basins. Thus, these processes highly influence the resulting sequence stratigraphy, resulting in some characteristic stacking patterns (Zavala et al., 2024). Based on the balance between the accommodation space and the sediment plus water supply, Carroll and Bohacs (1999) recognised three types of lake, termed overfilled, underfilled, and balanced-fill. Each lake type is characterised by different lake-level variations. In overfilled lakes, the lake level is near stable, since it is controlled by the spill point. Conversely, the underfilled stage shows the maximum rates of lake-level changes, drastically fluctuating below the spill point. Among these two opposite situations, balanced-fill lakes represent an intermediate condition in which the lake level can be periodically below or at the spill point. Each lake type is characterised by a specific stacking pattern, hydrology, and facies association (Zavala et al., 2024). All these features strongly influence the nature (i.e. autochthonous vs allochthonous) and preservation of the organic matter accumulated in lacustrine systems. Despite the fact that lacustrine deposits have been the subject of numerous palynological contributions, most studies do not consider these lake categories to analyse the origin and taphonomy of the recovered organic matter. Thus, the information on how palaeoenvironmental conditions – such as redox conditions, water pH, and input of terrestrial components – influence the amount, type, and preservation of the accumulated organic components in these different types of lake is very scarce (e.g. Bohacs, 2012).

In this contribution, a complete lacustrine succession from the Jurassic of extra-Andean Central Patagonia, Argentina, is analysed from palynological and sequence-stratigraphy viewpoints. This study is based on the detailed analysis of 51 samples from the late Early to Middle Jurassic Cañadón Asfalto Formation (Stipanicic et al., 1968) outcropping in the Cerro Cóndor area (Fig. 1). The integration of palynological results with sedimentological and sequence-stratigraphic analyses allowed us for the first time to understand the influence of the different lake stages in the origin and preservation of organic matter. This study approaches the analysis of the total acid-resistant organic content (palynofacies analysis) recovered from the samples studied here. This technique in combination with data from organic geochemistry constitute an excellent tool to aid the hydrocarbon source rock potential of the studied formations (e.g. Batten, 1996; Suarez-Ruiz et al., 2012). The goals of this contribution are (i) to understand the evolution and sequence stratigraphy of the Cañadón Asfalto Formation, mainly based on palynofacies and sedimentological analyses, (ii) to identify the origin and taphonomic attributes of the organic matter accumulated during the different lake's stages, and (iii) to evaluate the source-rock potential of the analysed rocks based on palynofacies combined with data from organic geochemistry (i.e. total organic carbon, or "TOC").

2 Geological setting

The Cañadón Asfalto Basin is the result of a complex tectonic evolution, developed between the Early Jurassic and the Late Cretaceous, related to the break-up of Gondwana (Figari et al., 2015). This basin was configured after a mechanic subsidence along north-westerly oriented strike half-grabens that defined isolated depocentres as part of a major rift zone (Cabaleri and Benavente, 2013; Figari et al., 2015). At present, there is no overall agreement on the number of existing depocentres. As an example, Silva Nieto et al. (2007) defined three depocentres, while Figari et al. (2015, and bibliography therein) recognised six. Silva Nieto et al. (2003) and Cabaleri et al. (2010) subdivided the Cañadón Asfalto Formation into two members, termed (from base to top) Las Chacritas and Puesto Almada. The Las Chacritas Member comprises lacustrine sediments with volcanic intercalations at the base, while the Puesto Almada Member, mainly composed of coarser siliciclastic sediments, is interpreted as a fluvial progradation towards the lacustrine environment. Conversely, Figari et al. (2015, and bibliography therein) did not recognise such a subdivision for the Cañadón Asfalto Formation and grouped the depocentre infill into three unconformity-bounded megasequences, termed J_1, J_2, and K. These megasequences overly a Paleozoic basement composed of schists and granitoids from the Cushamen (Volkheimer, 1964) and Mamil Choique (Ravaz-

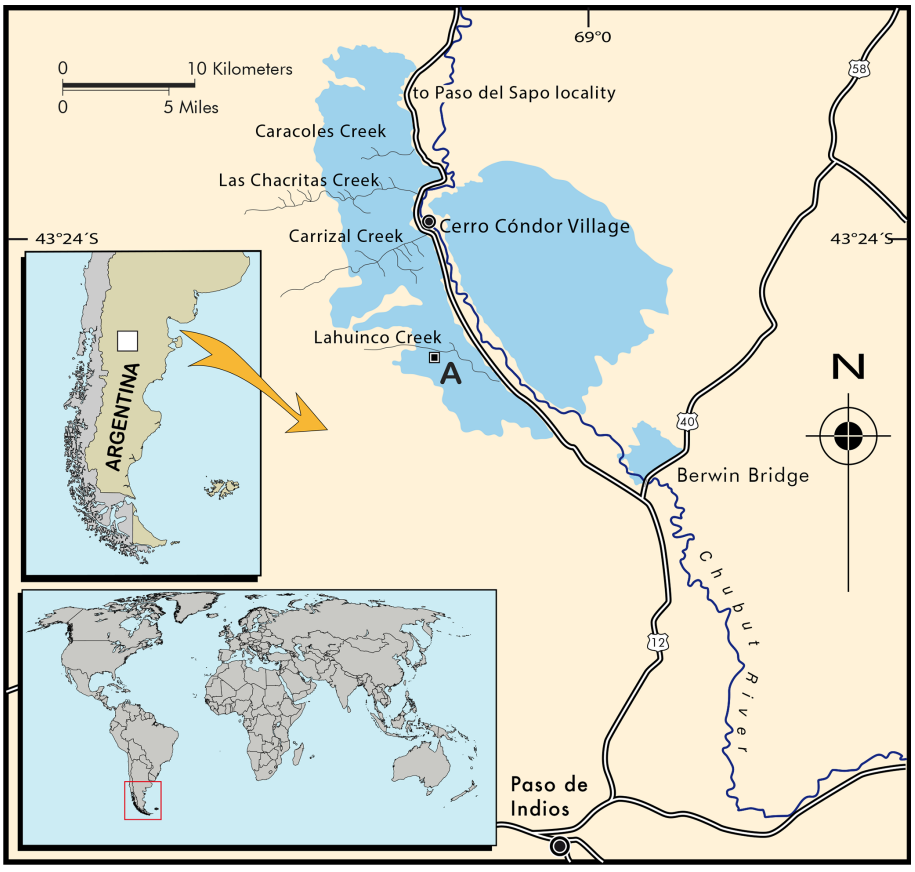

Figure 1. Location map with an indication of the Jurassic outcrops of the Cañadón Asfalto Formation at the Cerro Cóndor depocentre, area of the middle Chubut River valley, Patagonia, Argentina (adapted from Olivera et al., 2015). (A) Location of the Cañadón Lahuincó "A" section.

zoli and Sesana, 1977) formations. The J_1 megasequence encompasses the Las Leoneras (Nakayama, 1973), Lonco Trapial (Nullo and Proserpio, 1975; Pankhurst et al., 1998; Di Capua and Scasso, 2020), and Cañadón Asfalto (Stipanicic et al., 1968) formations. These units mostly show transitional contacts between them, although some angular unconformities and/or erosive boundaries are locally recognised because of their accumulation in a tectonically-active volcanic environment. The older unit, the Las Leoneras Formation, comprises alluvial, fluvial, and lacustrine metasediments and pyroclastic rocks assigned to the earliest Early Jurassic (Cúneo et al., 2013). This basal succession is covered by the Pliensbachian–Toarcian volcanic and volcaniclastic deposits of the Lonco Trapial Formation (Cúneo et al., 2013). Overlying these deposits, the late Early–Middle Jurassic Cañadón Asfalto Formation is recognised. The age of this unit is constrained between the Late Toarcian and the Late Bajocian based on biostratigraphically useful palynomorph species (Olivera, 2012; Olivera et al., 2015). This stratigraphic framework is supported by the result of a high-precision U-Pb zircon age (suggesting an early–middle Toarcian age; Cúneo et al., 2013). The Cañadón Asfalto Formation is in turn overlain by the J_2 megasequence, which comprises the Oxfordian–Kimmeridgian Cañadón Calcáreo Formation (Proserpio, 1987), composed of a thick succession of alluvial and lacustrine sediments (Cúneo et al., 2013; Figari et al., 2015). These megasequences are unconformably overlain by the fluvial and lacustrine Cretaceous deposits of the Chubut Group (K megasequence).

3 Materials and methods

3.1 Stratigraphic section and data collection

A 323 m thick stratigraphic section was measured, described, analysed, and sampled in detail at the Cañadón Lahuincó "A" section (43°30′59″ S, 69°08′20″ W), which is located in the Cerro Cóndor depocentre (Figs. 1 and 2). This section was measured in detail bed by bed, using a Jacob staff, and positioned by a GPS. Each bed was carefully described, with particular attention paid to the primary characteristics, such as lithology, sedimentary structures, grading, bedding contacts, bed geometry, trace fossils, presence of body fossils, and colour. This description was complemented by a de-

tailed rock sampling for palynological studies. The detailed description allows one to perform a facies analysis, focused on recognising the active sedimentary processes during the deposition (facies) and depositional environments (facies associations and sequences). The analysis of the different hierarchically order stacking patterns allows us to review the lake evolution from a sedimentological and stratigraphic point of view.

3.2 Sampling and laboratory treatment

A total of 51 outcrop palynological samples of very fine-grained and fine-grained sandstones and siltstones from the Cañadón Asfalto Formation were studied (Fig. 2). These samples were prepared according to standard palynological techniques, using non-oxidative acids (i.e. hydrochloric and hydrofluoric acids) to avoid affecting the natural colour of the organic components and the fluorescence of the hydrogen-rich particles (e.g. Tyson, 1995; Oboh-Ikuenobe and de Villiers, 2003). Two slides were mounted, the first made after the treatment with the hydrochloric and hydrofluoric acids to evaluate the total organic content, and the second following sieving the organic residue using a 10 µm mesh, leading to performing the palynofacies count (Batten, 1983; Batten and Morrison, 1983). The total organic carbon (TOC) analysis of selective 25 samples were performed in LABSPA (Soil, Plant and Environment Analytical Services) CONICET (Consejo Nacional de Investigaciones Científicas y Técnicas)/UNS (Universidad Nacional del Sur), Bahía Blanca city, Buenos Aires province, Argentina. The evaluation of the samples according to their carbon richness expressed by TOC in weight per cent (wt %) provides useful information on hydrocarbon source rock potential. The palynological slides are housed in the Paleontological Museum Edigio Feruglio Repository, Trelew city, Chubut province, Argentina. They are identified by the catalogue number, preceded by the abbreviation MPEF-PALIN (Museo Paleontológico Edigio Feruglio, Palinología). The location of the different identified components of the palynological matter (PM) are referred to by England Finder coordinates (EFcos).

3.3 Palynofacial analysis and statistical techniques

A palynofacies is defined as a distinctive palynological matter (PM) assemblage thought to reflect a specific set of environmental conditions or to be associated with a characteristic range of hydrocarbon-generating potential (Tyson, 1995, p. 4). Therefore, the integral palynofacies study involves not only the identification and quantification of the different organic components but also the description of the features of each one (i.e. size, shape, colour, and state of preservation). In this contribution, the evaluation of the PM was made considering two major categories (Table 1): (1) structured organic matter (i.e. palynomorphs, translucent, and opaque phytoclasts) and (2) unstructured organic matter

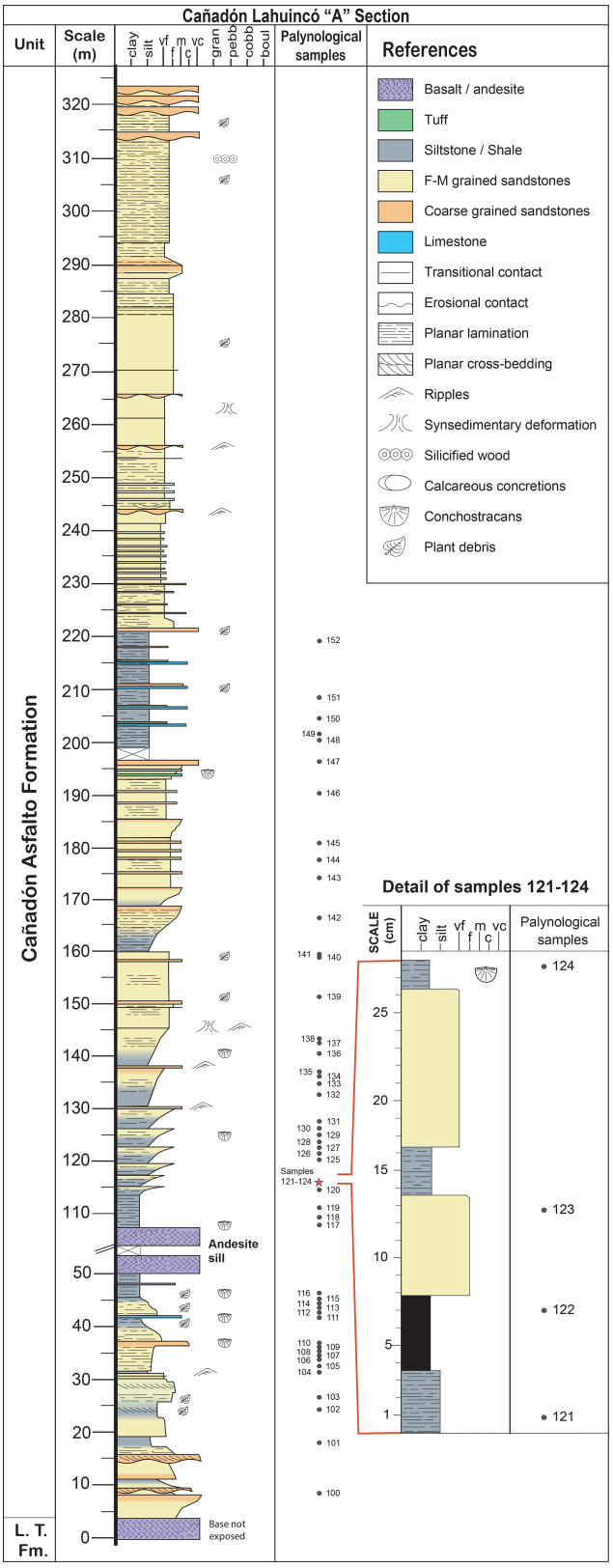

Figure 2. Stratigraphic column of Cañadón Lahuincó "A" section showing the sedimentological and fossil characteristics, with an indication of the studied palynological samples L.T. Fm: Lonco Trapial Formation.

(i.e. amorphous organic matter). The different organic particles were classified using terminology adapted from Batten (1983, 1996), Tyson (1995), and Oboh-Ikuenobe and de Villiers (2003). Cuticles and tracheids are very scarce; therefore, to avoid obscuring the meaningful information and/or real trend of this dataset with noise data, this type of particle has been added up to the woody remains under the "biostructured phytoclasts" category (Table 1). In order to quantify the relative abundance of each palynofacies component, a minimum of 500 particles were counted per sample under transmitted light (TL) microscopy (Olympus BX40). Based on their biological affinities, palynomorphs were classified into six major groups: lycophyte and fern spores, Pteridospermales and Coniferales pollen grains, Chlorophyta algae (Table 2), and fungal spores. A list of the identified palynomorph species is presented in Appendix A. The palynological count considered between 250 and 400 specimens per palynomorph's productive sample. Details of these statistical results were published in Olivera et al. (2015) and are shown in Table S1 in this contribution. The relative frequency (%) diagrams were calculated using TGview 2.0.2 (Grimm, 2004). Palynofacies data were interpreted using the multivariate statistical program PAST (PAleontological STatistics) by Hammer et al. (2001).

In order to form groupings of samples with a similar composition of PM (palynofacies type), cluster analysis (Q-mode) was selected as the most appropriate multivariate analytical method for this dataset. It was performed with the Euclidean distance and the unweighted pair group method (UPGM). The cluster analysis graphics indicate the cophenetic correlation. It is defined as the linear correlation coefficient between the cophenetic distances obtained from the dendrogram and the original distances (or dissimilarities) used to construct this graphic (Anderberg, 1973; Kovach, 1989). The magnitude of this coefficient should be close to 1 for a high-quality solution.

In addition, a palynofacies parameter, i.e. equidimensional : blade-shaped opaque particles (eo : bo) ratio, was considered.

The palynological samples were systematically examined on a standard magnification (×20 objective), under reflected fluorescence light microscope (RFL; Olympus BH2) in order to assess their preservation state and to improve the taxonomic palynological determinations (Tyson, 1995). In those samples with palynomorph content, the colour of the PM was qualitatively assessed applying the thermal alteration index (TAI) method (Staplin, 1969; Pearson, 1990), with the aim of estimating the thermal maturity of the PM. Psilate pollen grains belonging to the *Inaperturopollenites* Pflug and Thomson fossil-genus were selected for the measurement of the colour of palynomorphs on account of the relatively uniform thickness of its exine. In order to avoid a potential misinterpretation of the colour data caused by unusual thickening resulting from taphonomic folding, only the unfolded areas of the grains were considered. Based on the relative frequencies and fluorescence characteristics (i.e. relative intensity, colour, and heterogeneity) of the PM, the palynofacies assemblages were classified into four main kerogen types: essentially inert material (Type IV), gas-prone material (Type III), oil-prone material (Type II), and highly oil-prone material (Type I) according to Tyson (1995, p. 344).

4 Results

4.1 Sedimentology and sedimentary cycles

A total thickness of 323 m of the stratigraphic section was described, sampled and analysed in detail in the Cañadón Lahuincó "A" section (Fig. 2). The lower part of the section is composed of an overall fining – and thinning – upward clastic succession extended up to about 112 m from the base. Internally, this lower interval shows several fining-upward cycles of up to 10 m thick. These cycles conform elementary depositional sequences (Zavala et al., 2024), commonly starting with coarse-grained sandstones and ending with fine-grained (silty-shale) deposits with abundant plant remains and conchostracan valves (Fig. 2). At 45 m from the base, the section is almost entirely composed of black shales. This shale interval is intruded by a more than 50 m thick andesite sill. At roughly 112 m from the base, this basal interval is in turn followed by an overall coarsening-upward succession (Fig. 2), extending up to 198 m from the base (Fig. 2). This succession is composed of shale and fine- to coarse-grained sandstone deposits commonly showing interbedded thin tuff levels. Internally, these deposits compose simple or coarsening-upward parasequences (Van Wagoner et al., 1990) up to 15 m thick, commonly showing abundant plant remains. Mudstone beds commonly bear conchostracan valves (Fig. 2). After a cover interval of about 2 m, the section continues with a fine-grained succession of shales with minor sandstone and limestone beds, each up to 40 cm thick (Fig. 2). At about 221 m from the base, the shales are sharply overlaid by fine- to coarse-grained sandstones, mostly composing coarsening-upward cycles up to 30 m thick, with abundant tractive structures and plant remains. This sandy succession is extended up to the top of the section, showing an overall progradational trend composing a progradational parasequence set (Van Wagoner et al., 1990).

4.2 Palynofacies analysis

The most conspicuous feature of the PM recognised in Cañadón Lahuincó "A" section is the dominance of terrestrial material, mainly phytoclasts (between 31 % and 100 % of the total PM; Figs. 3–5). However, considering the relative variations of each individual PM's category (Tables 1 and S2), four palynofacies types (A–D), and one outlier sample (MPEF-PALIN117) emerge from the cluster analysis (Fig. 6). The cophenetic correlation coefficient of the dendrogram graphic is 0.735.

Table 1. Classification of the identified palynological matter with source affinity indications. Principal source of information from Batten (1983), Tyson (1995), Oboh-Ikuenobe and de Villiers (2003), and Olivera (2012).

Major categories	Categories		Description	Source	
Structured palynological organic matter	Palynomorphs	Sporomorphs		Spores and pollen grains	Reproductive structures of vascular land plants
		Organic-walled phytoplankton		Freshwater algae	Chlorophyte algae
	Phytoclasts	Translucent (at least at edge)	Wood	Particles lath-shaped with bio-structure; sometimes these cellular features are only partially visible	Macrophyte plant debris
			Tracheid with pits	Lignified fragments having bordered holes or "pits"	
			Tracheid without pits	Lignified fragments having ± length-parallel stripes or bands without visible pits	
			Yellow-brown fragment	Particles angular in shape, yellow or orange to pale brown in colour and small in size; without biological structures	
			Black-brown fragment	Particles angular in shape, dark-brown to almost black in colour and small in size; without biological structures	
		Opaque (Opaque up to edge, non-fluorescent)	Blade-shaped	Elongate particles, without biological structures, variable in size	
			Equidimensional	± Equidimensional particles, without biological structures, variable in size	
Unstructured organic matter	Amorphous organic matter (AOM)		Spongy	Masses with homogeneous aspect, orange-brown to pale or dark-brown in colour	Mainly derived from degradation of continental algae
			Fibrous	Masses with typical internal fibres, orange-brown to pale or dark-brown in colour	Mainly derived from degradation of macrophyte tissues (in Olivera, 2012)
			Granular	Masses with clotted and typical solid inclusions	Phytoplankton or bacterially derived

Table 2. Biological affinities of spores, pollen, and organic-walled microplankton from the Cañadón Asfalto Formation. Sources of information concerning the natural relationships of palynomorphs: Dettmann (1963), Filatoff (1975), De Jersey and Raine (1990), Balme (1995), Sajjadi and Playford (2002), McKellar (1998), and Martínez et al. (2008a).

Division	Class	Order	Family	Fossil-genera
Tracheophyta	Lycopsida	Selaginellales/ Lycopodiales	Selaginellaceae/ Lycopodiaceae	*Retitriletes*, *Staplinisporites*
	Filicopsida	Filicales	Cyatheaceae/Dicksoniaceae	*Deltoidospora* *Dictyophyllidites*
			Dipteridaceae/Matoniaceae	
			Dicksoniaceae	*Granulatisporites*
			Osmundaceae	*Osmundacidites*
			Schizaeaceae	*Klukisporites*, *Ischyosporites*
	Gymnospermopsida	Pteridospermales	Corystospermaceae	*Alisporites*
			Caytoniaceae	*Vitreisporites*
		Coniferales	Araucariaceae	*Inaperturopollenites*, *Araucariacites*, *Callialasporites*
			Hirmerellaceae	*Classopollis*
			Pinaceae	*Indusiisporites*,
				Cerebropollenites
			Podocarpaceae	*Podocarpidites*, *Microcachryidites*, *Podosporites*, *Trisaccites*
Chlorophyta	Trebouxiophyceae		Botryococcaceae	*Botryococcus*

4.2.1 Palynofacies type A (PT-A) (Fig. 6)

This PT is characterised by the dominance of phytoclasts, varying from 61.3 % to 100 % of the total PM. Among this group, the translucent particles are the most abundant (Fig. 7a, Table S2). Based on the relative frequencies of the translucent and opaque phytoclasts, this PT is separated into two sub-palynofacies types, namely PT-A1 and PT-A2 (Fig. 6). The PT-A1, mainly recovered from very fine-grained sandstones and siltstones (Figs. 3–5), presents the relatively highest values of opaque particles of both sub-palynofacies types, especially lath-shaped ones (up to ∼ 42 %) (Fig. 7b, Table S2). The palynomorphs exhibit in general low percentages (0 % to 17.7 %) and a high degree of degradation (chemical oxidation sensu; Delcourt and Delcourt, 1980). The poorly preserved algal colonies are the unique palynomorphs identified in the Lower Cañadón Lahuincó "A" section. Conversely, above the volcanic sill, sporomorphs (i.e. spores and pollen grains) dominate the assemblages, especially pollen grains of Cheirolepidiaceae and Araucariaceae (Fig. 7c and d). While their percentages are relatively low, the podocarpacean pollen grains (Fig. 7e) reach the highest frequencies among all the Cañadón Lahuincó "A" levels studied here (2.8 %–5.5 %). The scarcely recognised organic-walled microplankton (OWM) is represented by *Botryococcus* colonies (chlorophytic algae). The palynomorphs are dark-yellow in colour when are observed under a TL microscope (TAI: 2+; Fig. 7d). Conversely, the PT-A2, mainly recovered from fine-grained sandstone levels, shows the highest frequencies of translucent phytoclasts in the studied section (Fig. 7f). Among them predominate the black-brown fragments with rounded edges (up to 55 % of the total PM; Fig. 7f). The scarcely identified palynomorphs are represented by degraded dark *Botryococcus* colonies, only recognised under RFL microscopy. In both sub-palynofacies, the AOM is chiefly spongy (Tables 1 and S2) and has a weak fluorescence in a light-brown colour.

4.2.2 Palynofacies type B (PT-B) (Fig. 6)

Although the phytoclasts are the most abundant particles (between 44 % and 71 %), this PT shows the greatest abundance of well-preserved palynomorphs of all studied Cañadón

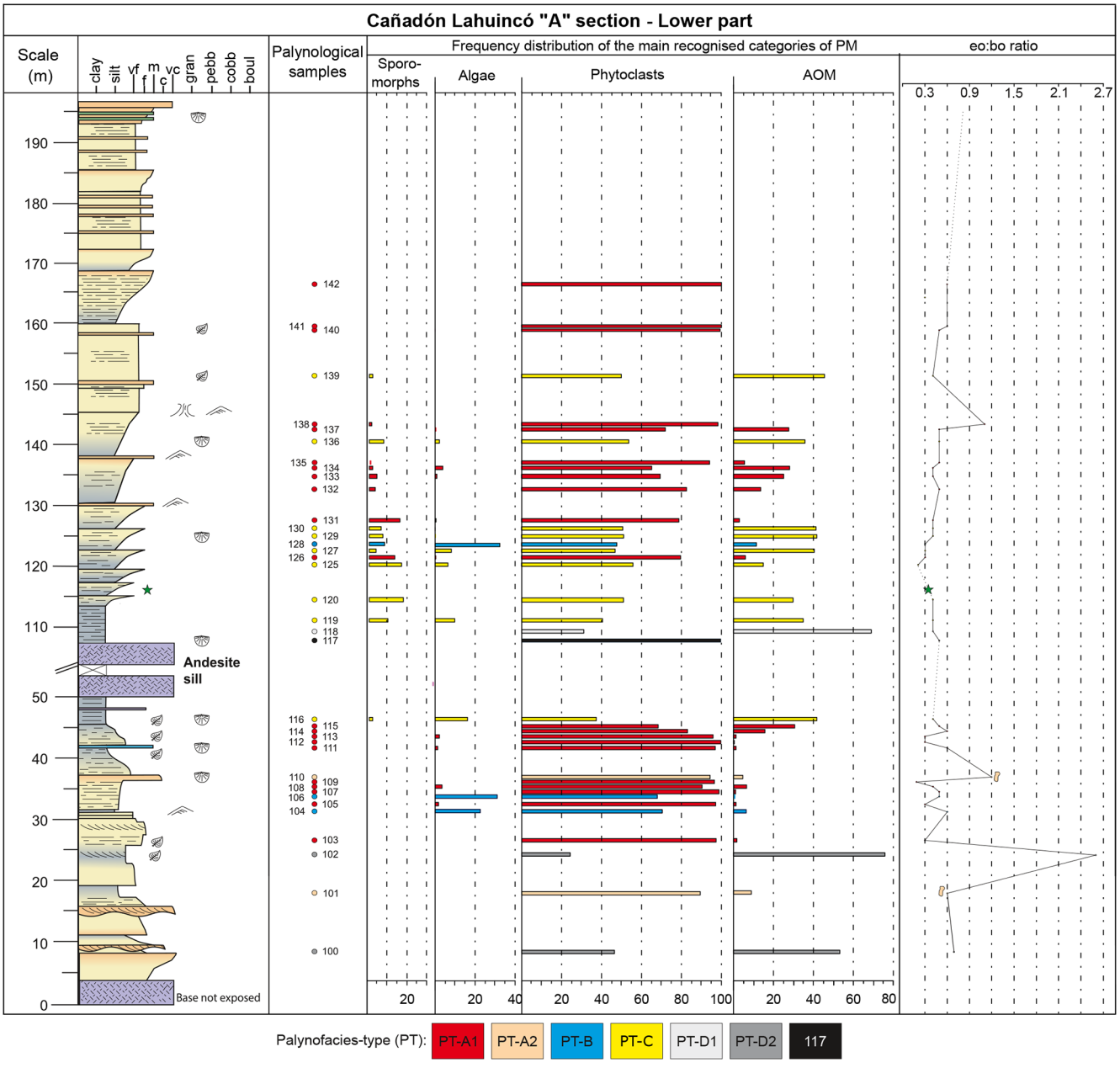

Figure 3. Quantitative distribution of major groups of the recognised palynological matter's categories in the Cañadón Asfalto Formation from the lower part of the Cañadón Lahuincó "A" section, expressed in percentages of total palynological matter based on the 51 studied samples.

Lahuincó "A" samples, reaching up to 40.2 % of the total PM spectrum (Figs. 3–5; Table S2). Among them, the OWM (i.e. *Botryococcus* colonies) is dominant. In the Lower Cañadón Lahuincó "A", only monospecific assemblages of *Botryococcus* colonies are recognised (Figs. 3 and 7g; Table S1), whereas in the assemblages towards the top of the section (i.e. MPEF-PALIN123/128 samples) terrestrial palynomorphs are incorporated, always subordinate to the algal material (Figs. 3, 4, and 7h; Table S1). The excellent state of preservation of the algal colonies is reflected in the strong yellow fluorescence that they show (Fig. 7i, j). Among the sporomorphs, only pollen grains have been registered. The Hirmerellaceae and Araucariaceae families are the most abundant, while the other recognised families (Pinaceae, Podocarpaceae, and Corystospermaceae) are present in very low proportions (< 2 %; Table S1). The phytoclasts are predominantly composed of translucent particles (25.23 %–43.45 %), mainly black-brown fragments (Tables 1 and S2). Among the opaque category, the blade-shaped particles (9.5 %–18.6 %) are predominant. The AOM is mainly

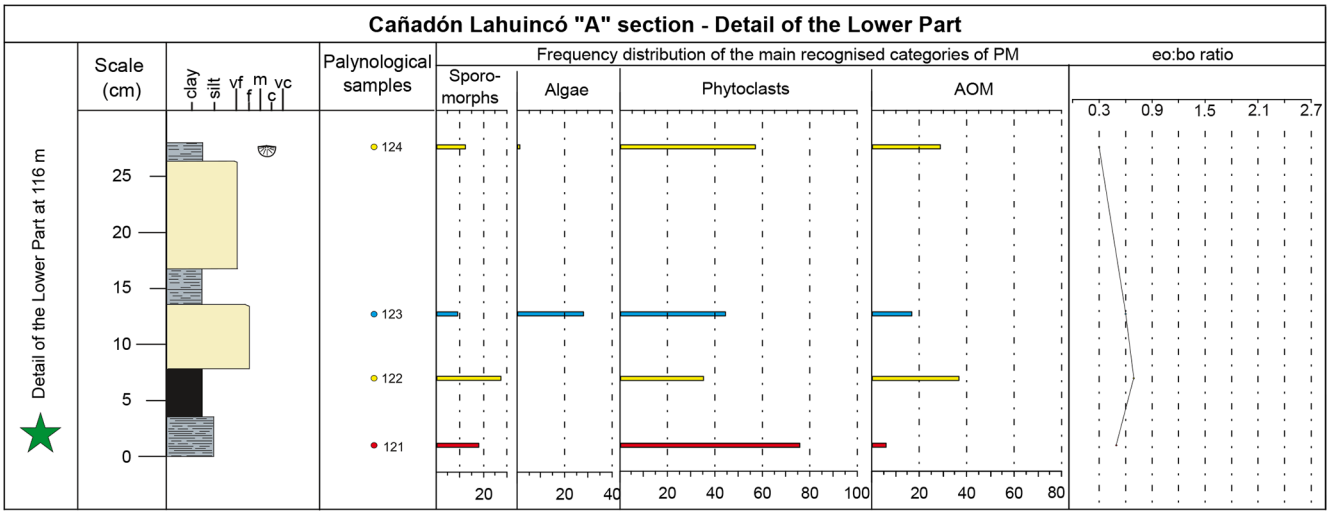

Figure 4. Detail of frequency distribution of the different recognised categories of palynological matter from MPEF-PALIN121 to MPEF-PALIN124 samples. (For interpretation of the references to colour in this figure legend, please refer to Fig. 3 of this article.)

of a spongy type, exhibiting heterogeneous fluorescence with a moderate to high intensity in a yellow to brownish-yellow colour (Fig. 7k, l).

4.2.3 Palynofacies type C (PT-C) (Fig. 6)

Despite phytoclasts representing the most abundant group (35.6 %–55.9 %), this PT is distinguished by presenting the highest frequencies of terrestrial palynomorphs observed in all studied Cañadón Lahuincó "A" samples (up to 27 %; Table S2). Sporomorphs (chiefly Hirmerellaceae and Araucariaceae pollen grains; Fig. 7m, n) are regularly present with percentages varying from 1.73 % to 27 % of the total PM; in addition, *Classopollis* tetrads and polyads were recognised (Fig. 7m, o). In general, the sporomorphs show a high degree of degradation and corrosion (sensu Delcourt and Delcourt, 1980) (Fig. 7n–p). The lowest percentages and the most poorly preserved terrestrial palynomorphs are recorded in the lower part of the section, which exhibits a thinning and fining-upward stacking pattern (Fig. 3, Table S1). Under TL microscopy, the palynomorphs show a pale-orange colour, coincident with a TAI value of 3– (Fig. 8a). Aquatic palynomorphs represented by *Botryococcus* colonies are present in low percentages (< 9.8 %), with a maximum of 16.35 % in the MPEF-PALIN116 sample (Fig. 3, Table S2). Despite the translucent phytoclasts are predominant in the major part of the samples belonging to this PT (17.6 %–35.8 %), the opaque, blade-shaped particles present relatively high values (14 %–28 %; Table S2). The AOM is predominantly of a fibrous type, comprising between 12 % and 45 % of the total PM (Table S2). It is characterised by weak to moderate fluorescence and pale to brownish-orange fluorescing colours (Fig. 8b, c). The well-preserved *Botryococcus* colonies in the MPEF-PALIN116 and MPEF-PALIN119 samples exhibit strong yellow fluorescence.

4.2.4 Palynofacies type D (PT-D) (Fig. 6)

AOM represents the dominant component of this PT, accounting for up to 75.6 % of the total PM spectrum (Fig. 3; Table S2). The three samples are barren in palynomorphs and, based on the phytoclast content, this PT was subdivided in two sub-palynofacies assemblages by the cluster analysis (Fig. 6). The PT-D1 presents the higher percentages of phytoclasts (31.3 %–46.5 %), mainly large blade-shaped opaque particles (Fig. 8d; Table S2). The AOM is predominantly spongy in aspect, reaching up to 69 % of the total PM. Conversely, the PT-D2 presents the lowest phytoclast concentration (24 %) and the highest proportion of dark-brown fibrous AOM (47.5 %) in all studied Cañadón Lahuincó "A" samples (Fig. 8e; Table S2). Among the phytoclasts, the translucent black-brown fragments are predominant, and the opaque particles are very scarce and relatively small in size (< 37 µm). In both samples, the PM is non-fluorescent.

4.2.5 Outlier sample, MPEF-PALIN117 (Fig. 6)

The most conspicuous feature of this sample is the great prevalence of opaque phytoclasts (86.9 %), predominantly comprising large blade-shaped particles (up to 200 µm; Fig. 8f). The remaining 13.1 % is represented almost exclusively by black-brown fragments (Table S2).

4.3 Total organic carbon

The range of TOC in the entire dataset varies from 0.13 % (PT-D1) to 11.96 % (PT-C) (Fig. 9). The PT-D shows the lowest values of TOC among all studied samples (Fig. 9).

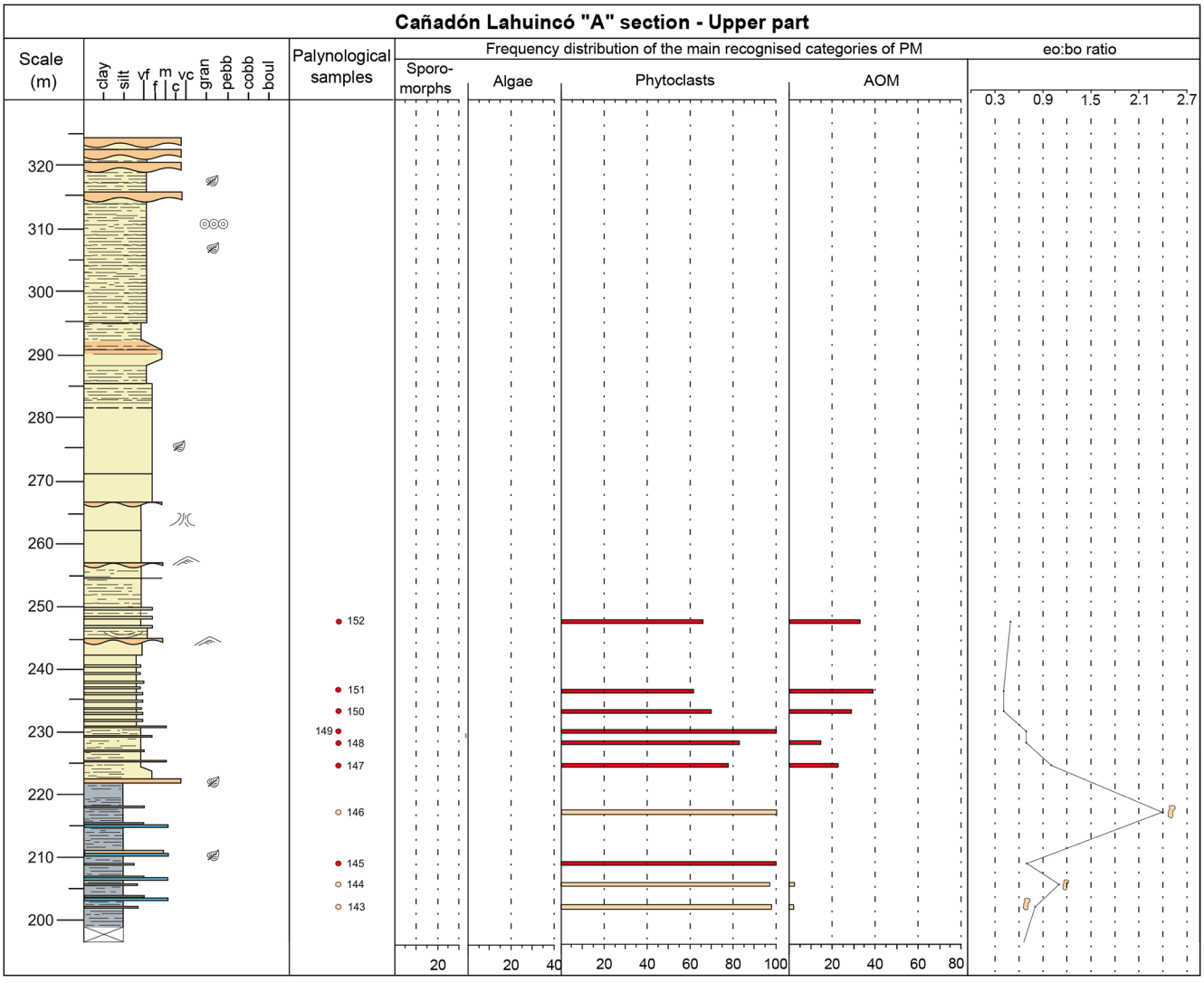

Figure 5. Quantitative distribution of major groups of the recognised palynological matter's categories in the Cañadón Asfal section, expressed in percentages of total palynological matter based on the 52 studied samples. (For interpretation of the references to colour in this figure legend, please refer to Fig. 3 of this article.)

Conversely, the PT-C presents the highest percentages of TOC registered in the samples studied here (Fig. 9), with an arithmetic mean of 6.43 %. The PT-B exhibits values that vary from 0.6 % to 4.3 % (Fig. 9), with an arithmetic mean of 2.9 %. The PT-A1 shows the higher values of the two defined sub-palynofacies, with an arithmetic mean of 1.55 %, while in the PT-A2 the average is 0.734 %. The MPEF-PALIN117 sample, widely dominated by opaque phytoclasts, shows a TOC of 2.04 %.

5 Discussion

5.1 Palaeoenvironmental reconstruction and sequence-stratigraphic analysis

Sedimentological and sequence-stratigraphic analysis of the Cañadón Lahuincó "A" section revealed the existence of two depositional sequences (termed Sequence I and Sequence II), each one characterised by specific lacustrine conditions (Fig. 10).

Sequence I is extended up to 197 m and displays a complete transgressive-regressive cycle (Figs. 10e and 11a). The lower part (TST) of Sequence I (0–112 m; Fig. 10) is characterised by different hierarchical ordered fining-upward cycles (Fig. 11a). Fining-upward cycles are the consequence of the introduction of a substantial volume of water and sediments

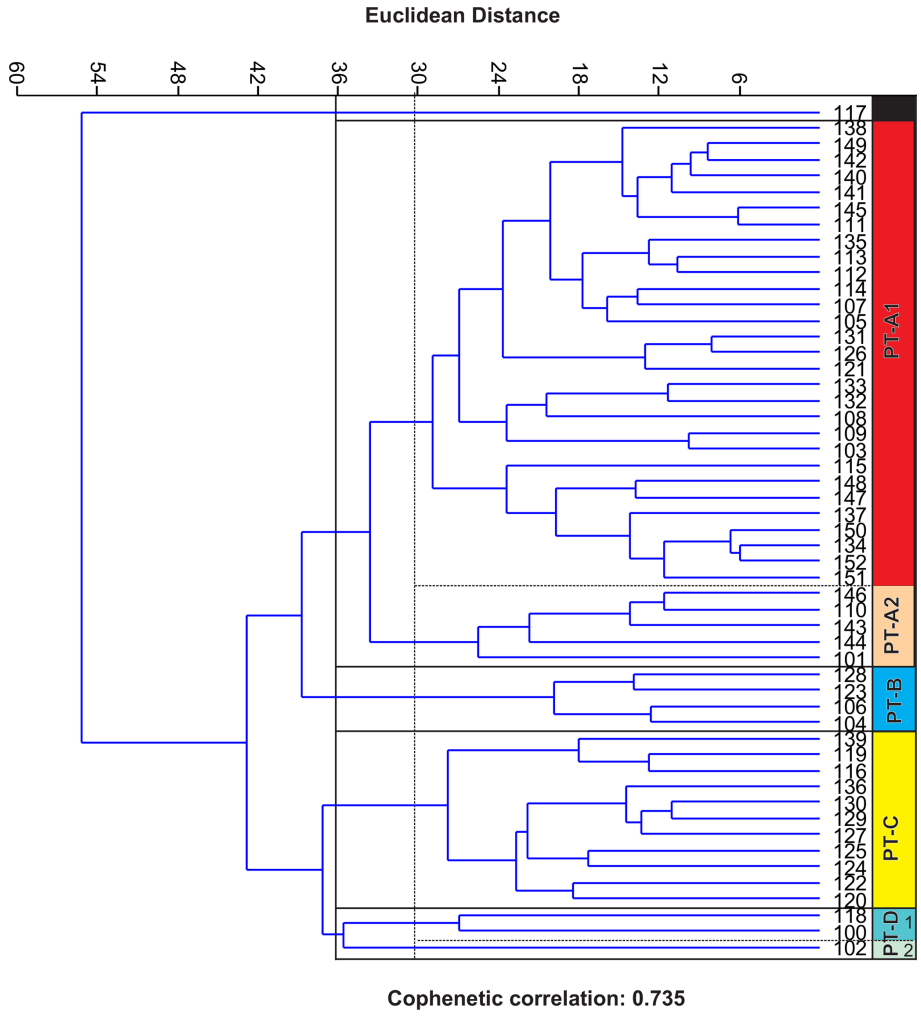

Figure 6. Cluster analysis, using Euclidean distance and the unweighted pair group method (UPGM), showing the grouping of the identified palynofacies type (PT) in the Cañadón Lahuincó "A" section.

in a hydrologically closed basin, resulting in an overall punctuated lake transgression. The smaller-scale cycles compose metres-thick normally graded deposits controlled by high-frequency transgressive-regressive climatic cycles (TST-RST in Fig. 10a, b). During these high-frequency transgressive cycles, lake waters dilute and rise during TST periods (Fig. 10a). In contrast, during periods of low water/sediment supply (RST; Fig. 10b), the lake-level falls, favouring the subaerial exposure of marginal areas during a forced regression, with the local development of arid palaeosols (Fig. 11b). The low sediment supply also contributed to creating restricted lake conditions, favouring phytoplanktonic primary productivity (Figs. 10b and 11c). This interpretation is in line with Cabaleri et al. (2005), Volkheimer et al. (2008), and Soreda (2012), who interpreted the lower part of the Cañadón Lahuincó creek's deposits as accumulated in a closed lake. According to the current paradigm of lacustrine sequence stratigraphy (Zavala et al., 2024), these fining-upward cycles evidence an accumulation in a transgressive system tract (TST; Fig. 10) of an underfilled lake, which is extended up to the maximum flooding surface (mfs; Fig. 10).

The upper part of Sequence I composes an overall thickening and coarsening-upward succession extended up to 197 m (Fig. 10). Internally, this interval shows multiple coarsening-upward cycles of different scales and hierarchies (Fig. 2). The existence of coarsening-upward cycles suggests a coastal progradation in a lake having a limited accommodation space. In clastic lakes, this coastal progradation is only possible with a near stable lake level, which suggests that the maximum lake level was effectively controlled by the spill-point. According to the sedimentological and stratigraphic evidence (Zavala et al., 2024), this interval is interpreted as accumulated during an overall regressive system tract (RST) in balanced-fill/overfilled lake conditions (Fig. 10c–e) by a stacked succession of littoral delta deposits (Fig. 11d–f). The interval located between 112 and 137 m is interpreted as ac-

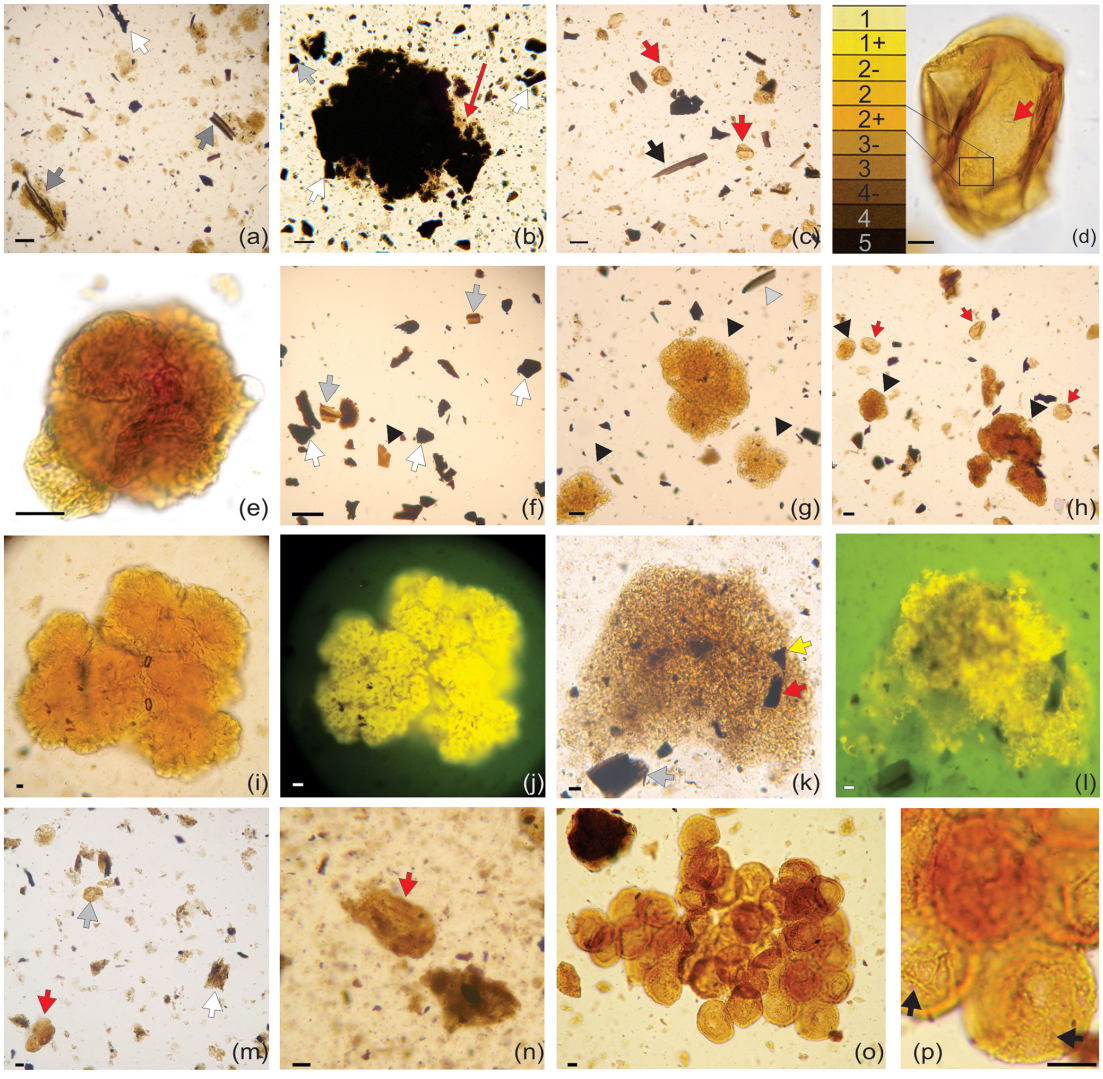

Figure 7. Palynofacies types and selected palynomorphs of the Cañadón Asfalto Formation from the Cañadón Lahuincó "A" section. **(a–e)** General view of PT-A1: **(a)** MPEF-PALIN151: H17/1. The grey arrows indicate tracheids without pits and the white arrow points out a blade-shaped opaque phytoclast. **(b)** MPEF-PALIN103: O28/2. The white arrow points out a blade-shaped opaque phytoclast, the grey arrow indicates an equidimensional opaque phytoclasts, and the red arrow points out a granular amorphous mass. **(c)** MPEF-PALIN121: V8/4. The red arrows indicate *Classopollis classoides* (Pflug) Pocock and Jansonius pollen grain, and the black arrow points out woody remains. **(d)** Table showing the spore colour index taken from Lucas and Omodolor (2018) (left), MPEF-PALIN133: Y27/0. *Inaperturopollenites giganteus* Góczán, the red arrow indicates a sector of thinner exine due to degradation, and the square indicates a sector of well-preserved exine (right). **(e)** MPEF-PALIN126: D28/2. *Podosporites variabilis* Sukh Dev. **(f)** General view of PT-A2; MPEF-PALIN101: N46/3. The white arrows point out black-brown fragments with rounded edges, and grey arrows indicate tracheids without pits. A yellow-brown fragment is indicated by a black head arrow. **(g–l)** General view of PT-B. **(g)** MPEF-PALIN106: D32/1. Compound colonies of *Botryococcus* sp. cf. *B. braunii* Kützing are indicated by black head arrows, and a tracheid without pits is pointed out by a grey head arrow. **(h)** MPEF-PALIN123: J49/3. The red arrows indicate *Classopollis* pollen grains, and the black head arrows point out *Botryococcus* sp. cf. *B. braunii* Kützing colonies. **(i, j)** MPEF-PALIN123: M29/3. Compound colony of *Botryococcus* sp. cf. *B. braunii* Kützing. **(j)** Reflected fluorescence light photomicrography. **(k, l)** MPEF-PALIN106: C24/1. Spongy AOM and phytoclasts. The red arrow indicates a blade-shaped opaque phytoclasts, the yellow arrow indicates an angular equidimensional opaque phytoclasts, and the grey arrow indicates a black-brown fragment. **(l)** Reflected fluorescence light photomicrography. **(m–p)** General view of PT-C. **(m)** MPEF-PALIN120: R54/3. Tetrad of *Classopollis* spp. is indicated by a red arrow, a highly degraded sporomorph is pointed out by a grey arrow, and a fibrous amorphous mass is indicated by a white arrow. **(n)** MPEF-PALIN119: K37/3. The red arrow indicates a highly degraded, partially amorphised araucariacean pollen grain. **(o–p)** MPEF-PALIN122: B46/3. *Classopollis* polyad infected by fungal spores of *Annella capitata* Srivastava. **(p)** Detail of *Classopollis* grains with the indication of fungal spores (black arrows). Scale bars: 10 µm.

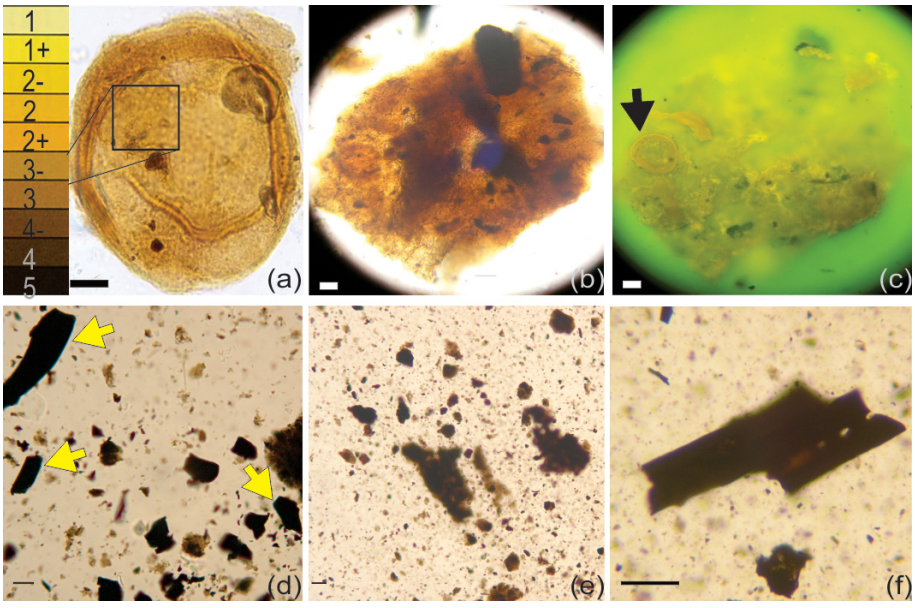

Figure 8. Palynofacies types and a selected palynomorph of Cañadón Asfalto Formation from Cañadón Lahuincó "A" section. **(a)** Table showing the spore colour index taken from Lucas and Omodolor (2018) (left), MPEF-PALIN122: A51/4. *Inaperturopollenites giganteus* Góczán, the square indicates a sector of well-preserved exine (right). **(b, c)** Fibrous amorphous mass; MPEF-PALIN130: P22/1. **(a)** Transmitted light microphotography. **(b)** Reflected fluorescence light photomicrography, with the black arrow indicating a *Classopollis* pollen grain masked by the amorphous mass. **(d)** General view of PT-D1. MPEF-PALIN118: N49/4. The yellow arrows indicate blade-shaped opaque phytoclasts. **(e)** Scale bar 30 µm, general view of PT-D2. MPEF-PALIN102: H46/4. **(f)** Scale bar 30 µm, general view of MPEF-PALIN117 outlier sample: T50/4. Scale bars: 10 µm, unless otherwise specified.

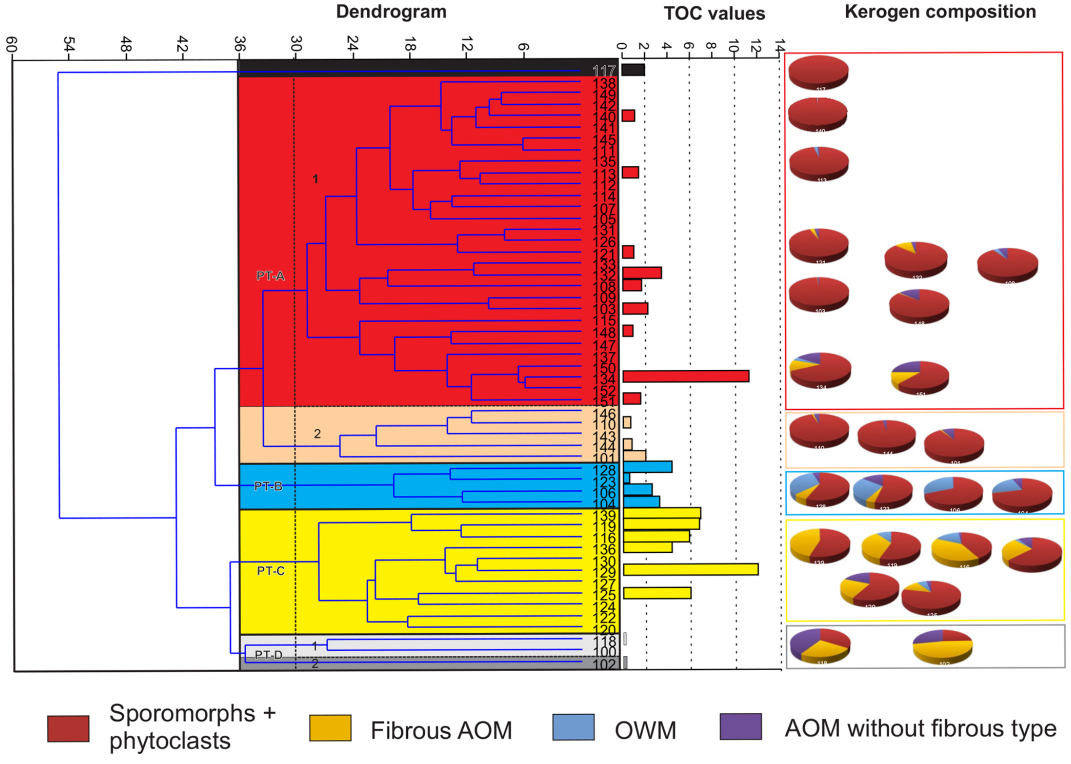

Figure 9. Cluster analysis graphic, with the total organic carbon percentages of each analysed sample represented as a bar (right). Pie charts show the kerogen composition of the selected samples (left). AOM: amorphous organic matter, OWM: organic-walled microplankton.

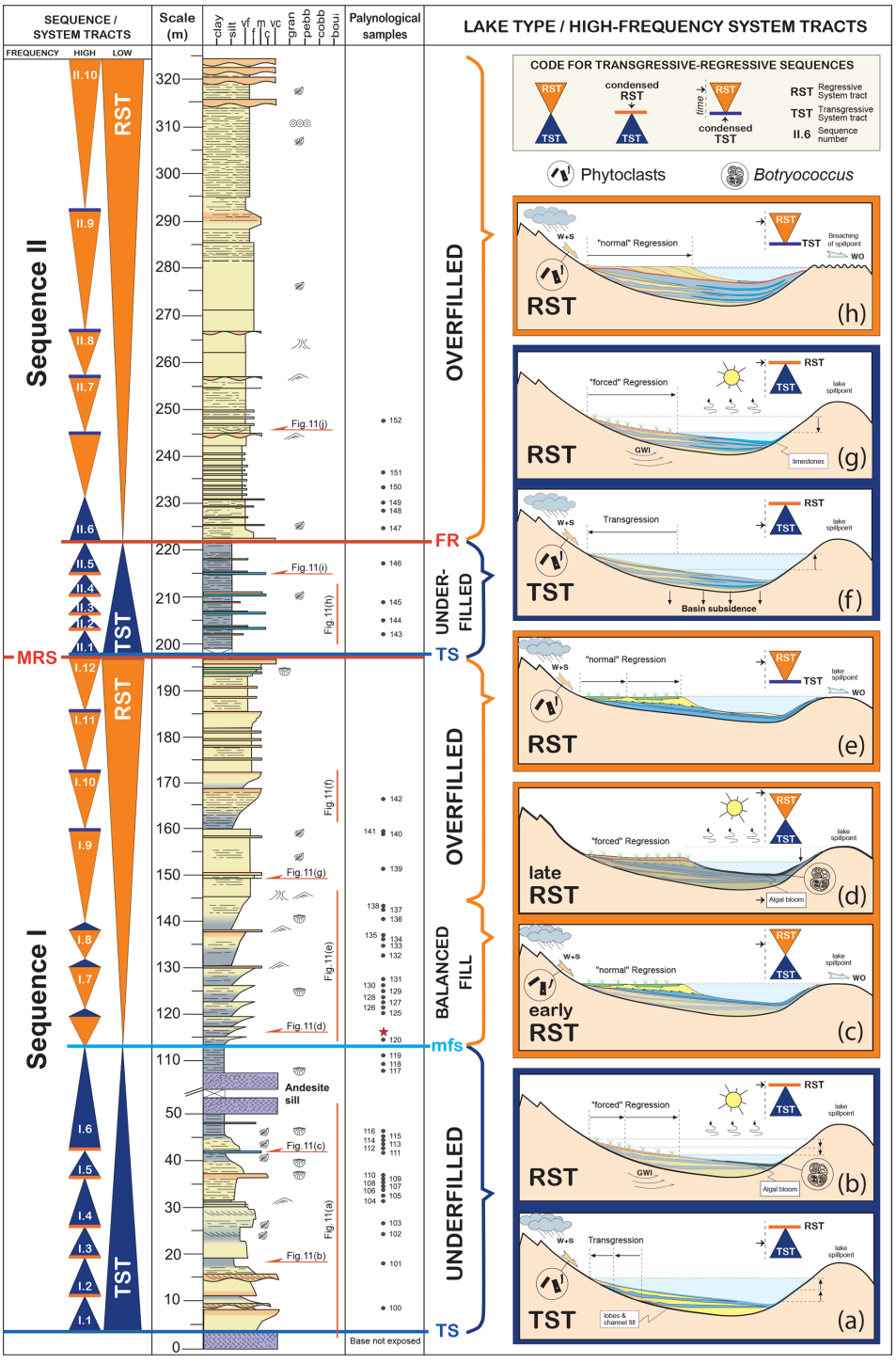

Figure 10. Integrated stratigraphic and conceptual model of lake-type evolution for the Jurassic Cañadón Asfalto Formation at the Cañadón Lahuincó "A" section. WO: water outflow; GWI: groundwater inflow. The measured stratigraphic column (left) is correlated with palynological sampling levels and key sequence-stratigraphic surfaces, including transgressive surfaces (TSs), maximum flooding surface (mfs), maximum regressive surface (MRS), and forced-regression surface (FR). Two depositional sequences (sequences I and II) are recognised and interpreted in terms of changing lacustrine hydrological balance. Conceptual panels (**a–h**, right) adapted from Zavala et al. (2024) illustrate the evolution from underfilled to balanced-fill and overfilled lake stages during transgressive (TST) and regressive (RST) system tracts, including normal and forced regressions, basin subsidence, breaching of the spillpoint, algal bloom development, and associated depositional processes (e.g. littoral delta progradation, channel-lobe systems, and limestone deposition). The figure highlights the tight coupling between lake-level behaviour, climatic forcing ($W + S$: water plus sediment supply), and sedimentary stacking patterns. The locations of the photographs shown in Fig. 11 are indicated in the stratigraphic column.

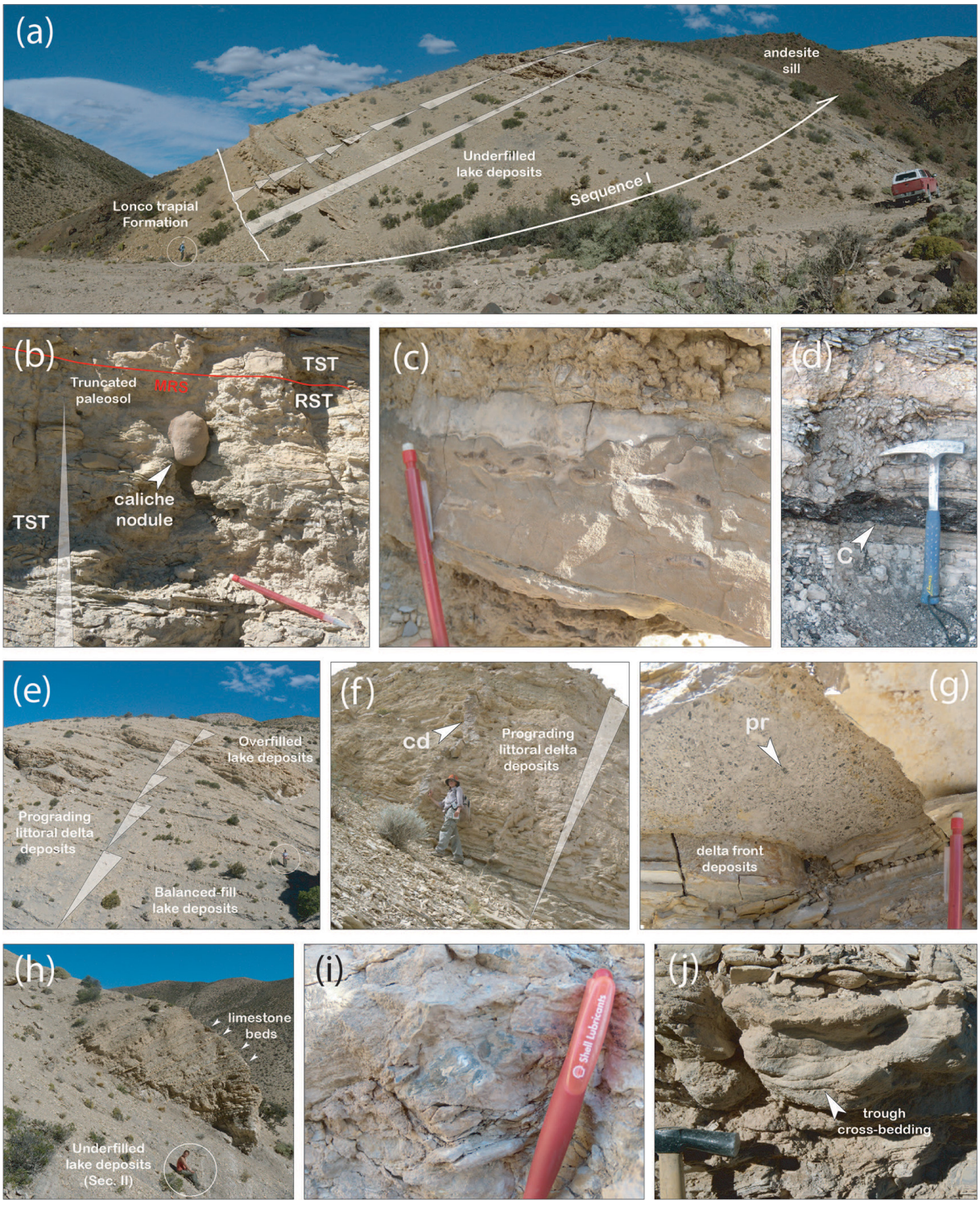

Figure 11. Some field examples of the Cañadón Asfalto Formation in the Cañadón Lahuincó "A" section. **(a)** Panoramic view of the lower part of Sequence I, characterised by fining and thinning upward cycles accumulated in an underfilled lake. **(b)** Detail of a palaeosol at the top of a high-frequency RST in underfilled lake deposits of Sequence I. **(c)** Limestone bed in the underfilled interval of Sequence I. **(d)** Thin coal bed in the balanced-fill interval of Sequence I. See the star in Fig. 2 for location. **(e)** Balanced-fill and overfilled intervals of Sequence I. Note the shallowing-upward cycles. **(f)** Detail of a coarsening and thickening-upward succession in Sequence I, interpreted as littoral delta deposits. **(g)** Plant remains in delta front deposits of Sequence I. **(h)** Fine-grained deposits with interbedded limestone beds. Underfilled interval, Sequence II. **(i)** Detail of the limestone beds. **(j)** Trough cross-bedded sandstones in littoral delta deposits in the overfilled interval of Sequence 2. The locations of these photographs are shown in Fig. 10.

cumulated in a balanced-fill lake (Fig. 10c), characterised by high-frequency climatic cycles, with alternating transgressions and delta progradations (TST – early RST; Figs. 10c and 11g) followed by a lake restriction (late RST; Fig. 10d). The last lake restrictions favoured the lacustrine primary productivity (Figs. 7g, h, and 10d). The upper part of the RST of Sequence I shows multiple progradational cycles with abundant plant remains, which suggests an accumulation in littoral delta systems in an overfilled lake (Fig. 10e). The RST of Sequence I is extended up to the maximum regressive surface (MRS), which marks the boundary with Sequence II. Sequence II shows an overall finning and then coarsening-upward succession extended up to the top of the section (324 m; Fig. 10). The basal boundary of Sequence II suggests the occurrence of a drastic change in the depositional conditions (paraconformity), evidenced by a sudden increase in basin accommodation, probably driven by an increase in tectonic subsidence. As a consequence, Sequence II starts with a basal shale interval (TST) composed of multiple small-scale cycles of shale interbedded with sandstone and limestone beds. These cycles suggest an accumulation in a partially restricted and closed lake (Fig. 11h, i). Sandstone and shale deposits are mostly associated with high-frequency transgressive periods (Fig. 10f). In contrast, limestone beds probably represent punctuated periods of lake restriction during high-frequency RST periods (Fig. 10f) with alkaline waters in an underfilled lake. This fine-grained interval is in turn sharply overlaid (222 m) by a dominantly sandy succession showing punctuated coarsening-upward cycles (Fig. 10). The basal sharp boundary with the RST of Sequence II is interpreted as a forced regression (FR), resulting from the breaching of the lake spillpoint and the onset into overfilled lake conditions (Zavala et al., 2024; Figs. 10h and 11j). The multiple coarsening-upward successions recognised in this upper section are interpreted as accumulated by progradational littoral deltas developed in an overfilled freshwater lake.

5.2 Palaeoenvironmental reconstruction and palaeoclimatic inferences based on palynofacies analysis

Despite the wide dominance of land-derived material, such as phytoclasts and fibrous AOM, in all the defined palynofacies types (Table S2) that indicate an overall high terrestrial input to the basin, the relative variations in the 12 PM categories (Table 1, Figs. 3–5) suggest the development of small-scale palaeoenvironmental changes into the major recognised sedimentary cycles (Fig. 10). The base of the underfilled succession (TST) of Sequence I is characterised by the intercalation of two PTs, i.e. PT-D and PT-A (Fig. 3). The PT-A shows the largest percentages of phytoclasts (up to 100 % of the total PM; Table S2) among all the defined PT, especially the assemblages belonging to the PT-A2 (Figs. 3 and 4). The PT-A2 PM was mainly recovered from fine-grained sandstone levels (Fig. 2). As previously noted by Fisher et al. (1979), the response of organic particles to bottom shear is usually similar to that of spheres of the same density, and the macrophyte debris have shown to present a similar hydrodynamic equivalence to coarse silt and fine sand. Among the phytoclast group, the black-brown fragments with rounded edges are dominant in this sub-palynofacies (Fig. 7f). High frequencies of dark-coloured rounded edge phytoclasts have been previously interpreted as recycled from older deposits and/or transported far from their source before deposition (e.g. Oboh-Ikuenobe and de Villiers, 2003; Falco et al., 2021; Chalabe et al., 2024). Furthermore, Tyson (1995) pointed out that woody material is selectively preserved and rounded by reworking in the bed load. In addition, the scant recognised AOM shows a poor degree of preservation (weak fluorescence), and the recovered palynomorphs are represented by highly degraded non-fluorescent *Botryococcus* colonies. The taphonomic attributes of *Botryococcus* were previously interpreted by Hutton et al. (1980) as the result of penecontemporaneous reworking, i.e. that which occurs over a relatively small time-scale (sensu Cushing, 1964). These features suggest the transport and accumulation of these deposits in a relatively high-energy oxidising environment. This could be related to the intensification of rainfall during a wetter period, leading to extraordinary fluvial discharges (i.e. hyperpycnal flows). The PT-A1, recovered from relatively finer lithologies (Figs. 3–5), shows a higher participation in the assemblages of opaque phytoclasts, mainly blade-shaped ones (Figs. 3–5, Table S2). Based on the physical and morphological characteristics of the equidimensional and blade-shaped opaque phytoclasts, variations in the eo : bo ratio values have been previously interpreted as variations in the flow velocity (Chalabe et al., 2022). When the flow velocity suffers a significant decrease, the relatively lighter, more buoyant material (i.e. blade-shaped opaque particles) is progressively accumulated by fallout. Thus, the PT-A1, which exhibits the lowest values of eo : bo ratio in the lower TST succession (Figs. 3–5, Table S2), could be related with its accumulation in relatively distal settings from a waning flow during the wetter season. Conversely, the PT-D shows a wide dominance of non-fluorescent AOM (Figs. 3 and 8d, e) and a high degree of degradation in all recovered PM. These features could indicate unfavourable environmental conditions for the preservation of the organic matter, with the selective destruction of the less resistant material. It could be related to the exhumation and reworking of these deposits in a context of high-energy fluvial discharges, mainly reflecting the taphonomic history of the palynological assemblages more than a specific depositional setting. However, the greater presence of blade-shaped, opaque phytoclasts in PT-D1 (MPEF-PALIN118) (Fig. 8d) could indicate their accumulation in a more distal position and/or a lower degree of progress in the rotting and coalification processes of the organic matter compared to PT-D2. This may be related to a change in the physical and chemical environmental conditions, at least at a local scale (e.g. more anoxic conditions in the pore spaces).

As the PT-A and, possibly, the PT-D, seem to indicate a wet period, the PT-B appears to reflect its accumulation during a drier one. This PT shows the highest values of highly fluorescent, well-preserved Botryococcaceae algae identified in all the studied samples (up to 32.38 % of the total PM) (Figs. 3, 5, and 7g–j). This algal family is a successful coloniser of shallow alkaline oligotrophic to mesotrophic waters under a wide range of climatic conditions throughout the year (Guy-Ohlson, 1992; Tyson 1995; Zippi, 1998). *Botryococcus* presents a series of adaptive strategies allowing its survival in some adverse conditions in which other types of algae cannot grow, such as the ability to store a large amount of reserve food and a type of wall that is resistant to desiccation (Guy-Ohlson, 1992). These features enable them to withstand relatively dry periods. Medeanic et al. (2010) documented wetter and drier periods in southern Brazil during the 20th century, based on algal palynomorph frequencies. They noted that the lowest sporomorph percentages and the complete *Botryococcus* predominance in the assemblages indicated drought periods. These authors pointed out that these intervals coincided with the lower water levels in the Mirim Lagoon and related them to variations in regional rainfall. Thus, the highest percentages of *Botryococcus* recorded in this study, along with a relative decrease in the phytoclast content (Figs. 3 and 5), could be interpreted as a drier period with an elevated evaporation rate and a decrease in the superficial run-off, which would have resulted in a contraction of the water body (Fig. 10b, d). In addition, these blooms (i.e. high primary productivity) would have produced oxygen-depleted conditions in the bottom waters (e.g. Papa et al., 2008; Fantasia et al., 2021), favouring the excellent preservation of the PT-B organic matter.

The PT-C shows transitional features between the PT-A and PT-B depositional conditions (Figs. 3 and 5). The lower frequencies of land-derived PM recorded in the PT-C assemblages compared to the PT-A (Table S2) suggest a reduced supply of water and sediments to the basin during the accumulation of these deposits. These drier climatic conditions are also indicated by a higher *Botryococcus* content and better preservation of the colonies (Figs. 3 and 5). Conversely, the PT-C assemblages exhibit a higher proportion of terrestrial material and a lower proportion of algae compared with the PT-B (Figs. 3 and 5), suggesting that the maximum aridity reflected in the PT-B PM had not yet been reached. In the upper part of the underfilled succession, an andesite sill body is identified (Fig. 2). The sample MPEF-PALIN117 comes from 1 m of this igneous rock. The recovered PM, which is dominated by dark particles, shows a high degree of oxidation (Fig. 8f). The high maturity and poor preservation of this organic matter may be attributed to the diagenetic effects of the intrusive emplacement.

A noteworthy feature of the underfilled palynological assemblages is the scant presence of land-derived palynomorphs (i.e. sporomorphs). Only two samples (MPEF-PALIN116 and MPEF-PALIN119, PT-C) show a low percentage of poorly preserved sporomorphs (1.73 % and 9 % of the total organic spectrum, respectively; Fig. 3). Behrensmeyer et al. (2000) pointed out that underfilled basins are not environments that enhance the preservation of land plant fossils. Nevertheless, compression-impression plant specimens with preserved organic tissues are recovered from levels located on the opposite side of the Cañadón Lahuincó creek that can chronocorrelated with this part of the section (Olivera et al., 2015, and bibliography therein). This may suggest that the chemical conditions of the underfilled lake's water (mainly pH conditions) would be highly unfavourable for the preservation of the sporopollenin, the organic compound that forms the sporomorph wall. The highly resistant biopolymer that composes the wall of the *Botryococcus* alga and the plant cuticles (e.g. Nip et al., 1986,; Zippi, 1998) could explain their presence in these deposits.

Overlying the basal TST of Sequence I, an RST is recognised, composed of balanced-fill/overfilled lake deposits (Fig. 10). The first noteworthy feature of the PT recovered from the finer-grained parasequences (between the MPEF-PALIN120 and MPEF-PALIN138 samples) is that the palynomorphs, and especially the sporomorphs, are present in nearly all the assemblages (Figs. 3 and 5, Table S2). The presence of this PM's group was such that enabled statistical counts (Table S1). Several authors have previously mentioned that the highest percentages of palynomorphs, and particularly the sporomorphs, are observed within the clay- to silt-size fraction as a consequence of its hydrodynamic equivalence with the fine quartz silt. Consequently, sediments comprising over 30 %–40 % sand-sized material generally exhibit lower sporomorph abundances (Tyson, 1995, and bibliography therein). Despite this, in the underfilled succession, siltstone levels were sampled, and in general no sporomorphs were recognised. As was previously discussed, this could be related to the physical-chemical characteristics of the water during the underfilled stage of the lake. Furthermore, the accumulation of the sporomorphs in different basin positions is related to the shape, size, and density of each sporomorph type. In general, all the PTs present high proportions of Hirmierellaceae pollen grains (i.e. *Classopollis* fossil genus), reaching $\sim$ 85 % of the total sporomorph group. The predominance of *Classopollis* in the palynological assemblages have been previously related to different factors, such as the primary productivity of the parental plants, the habitat in which they are thought to have developed (i.e. proximity to the site of deposition as marginal vegetation), and transportation sorting (Olivera et al., 2015, and bibliography therein). Nevertheless, it is noteworthy to mention that the PT-A1, which shows the highest percentage of land-derived organic components (phytoclasts plus sporomorphs), present a relatively high proportion of araucariacean pollen (up to 23.4 % of the total palynomorph group; Table S1). This pollen type has been previously considered as a water-transport palynomorph, because of the structural characteristic of its exine and its morphological features that enable it to be trans-

ported primarily via water (e.g. Caccavari, 2003; Holmes, 1994; Olivera et al., 2015, 2025). It reinforces the idea of the PT-A1 accumulation during periods with an increase in the water influx to the lake. In addition, it is interesting to highlight that the highest frequencies of Podocarpaceae pollen grains recorded here were found in two samples of the PT-A1 (MPEF-PALIN126 and MPEF-PALIN133; Fig. 7e). Saccate grains are generally associated with long-distance transport, particularly by wind, due to the presence of bladders that increase the pollen surface area while adding minimal mass (Schwendemann et al., 2007). Based on that, the relatively increase in the percentages of the saccate group is generally associated with accumulation in a relatively distal position (e.g. Tyson, 1995; Martínez et al., 2016). Thus, these two assemblages, which also show relatively low values of eo : bo ratio (Figs. 3–5), could be interpreted as accumulated in relatively more distal depositional settings.

Conversely, the PT-C exhibits the highest proportion of Hirmeriellaceae pollen grains recognised in all the PTs, along with a greater presence of tetrads and polyads (i.e. pollen grain agglomerates) of *Classopollis* (Fig. 7m, o). The record of tetrads and even polyads of any type of sporomorph has previously been considered as an indication of their accumulation near the source of vegetation (Maher, 2025, and bibliography therein). Moreover, the blade-shaped opaque phytoclasts present in these assemblages are larger than the equidimensional ones, which are regarded as more indicative of proximal positions (Tyson, 1995; Martínez et al., 2008b). All these features suggest the accumulation of this PM in a relatively proximal sub-environment of the lake system closer to the parental plants. The upward shallowing, progradational trend of the deposits (Fig. 2) yielding these assemblages, and the characteristics of these PM suggest its accumulation in a delta plain environment (Fig. 11f, g). The water characteristics of this particular depositional setting have been suggested as encouraging the development of fungal and bacterial aerobic biocenosis (Hart, 1994), and in general the palynomorphs identified in the PT-C exhibit a high degree of corrosion and degradation (Fig. 7n–p). The local accumulation of coal levels related to the swampy areas are previously pointed out as a common feature of the delta plain environment (Zavala et al., 2024), and the only coal level recognised in this study belongs to this PT (MPEF-PALIN122 sample; Figs. 4 and 11d). In addition, this assemblage presents the highest frequencies of *Annella capitata* Srivastava fungal spores identified in the samples studied herein (Fig. 7o, p).

In this part of the section, the PT-B shows a participation in the palynomorph assemblages of sporomorphs. Unlike the PT-C and PT-A1, these sporomorphs show an overall good degree of preservation. It could be a response to the development, at least temporarily, of the dysoxic to anoxic bottom-water conditions due to the algal bloom during drier periods (Fig. 10d). The presence of PT-B, and also the PT-C, in this first overall thickening and coarsening-upward succession (until sample 135) can be interpreted as showing fluctuating climatic conditions, i.e. wetter and drier periods. This palaeoenvironmental framework is in agreement with a balanced-fill lake stage (Fig. 10c, d), in which the PT-B would indicate the underfilled period (late RST) and the PT-A the overfilled one (TST – early RST; Fig. 10c, d). From this level upwards, the PT-B is not recognised, and the samples belonging to the PT-C only include a very low percentage of badly preserved algal colonies (Table S2). Thus, these palynomorph assemblages in the upper part of Sequence I could indicate the transition to an overfilled lake stage. From the MPEF-PALIN136 sample upwards to the section, the palynomorphs are only recorded in very low proportions in a few assemblages (Figs. 3 and 4). This may be related to the relatively coarser granulometry of these levels. The palynological assemblages recovered from Sequence II, after the MRS, belong to the PT-A (Figs. 4 and 10). The underfilled succession (TST) is characterised by the PT-A2 sub-palynofacies (Fig. 5), which would reflect the accumulation of these levels from relatively high-energy flows during intervals of rainfall intensification (i.e. wetter periods). In contrast, the limestone levels could indicate low clastic input to the lake during drier periods (punctuated by high-frequency RST; Figs. 10f and 11h, i). The PM assemblages recovered from the overfilled deposits belong to the PT-A1 (Fig. 5). This sub-palynofacies, which exhibits a relatively high proportion of opaque blade-shaped phytoclasts and weakly fluorescent AOM, could indicate more distal depositional settings and/or waning phases of the incoming fluvial flows. The unique presence of this sub-palynofacies in this part of the section, alongside the overall progradational trend of this succession, suggests a transition towards a more humid climatic condition during the infill of the lake.

5.3 Palaeoenvironmental conditions for the organic matter accumulation and source rock potential assessment of the Cañadón Asfalto Formation deposits

One of the primary stages in the study of a rock's hydrocarbon potential is the determination of its organic content. The TOC analysis is generally used as a proxy for determining this parameter. Despite the fact that TOC percentages are not strictly equivalent to the organic matter amount, it results in a very good approximation (Tyson, 1995, p. 81). Further discussion can be found in the literature explaining, or trying to explain, the different environmental factors that could condition TOC values (i.e. organic matter accumulation) with the main aim of predicting possible source hydrocarbon rocks (e.g. Tyson, 1989; Mustafa and Tyson, 2002; Li et al., 2021). The sediment granulometry and the predominant nature of the organic matter emerge as two important factors that condition the organic matter accumulation (Tyson, 1995, and bibliography therein). It is widely accepted that the finest lithologies contain higher TOC values than

the coarser ones, because of the organic components show similar settling velocities (i.e. hydraulic equivalence) to the fine-grained mineralic particles (in Tyson, 1995). When the percentages of TOC in the studied samples are observed in relation to the defined PTs, with the exception of one sample (i.e. MPEF-PALIN134, PT-A1), an overall trend can be distinguished (Fig. 9). The PT-D, dominated by non-fluorescent AOM (Figs. 3 and 9), exhibits the lowest TOC values, which are probably related to the accumulation of these palynological assemblages in a dynamic system, with sediment reworking under oxidising conditions that do not promote the preservation of the organic components. Conversely, the PT-C, followed by the PT-B, shows the highest TOC values registered in the samples studied here (Fig. 9). There is a general consensus that elevated percentages of TOC are related to low depositional rates that promote a minimal dilution of the organic matter with the clastic material (e.g. Tyson, 1995; Zavattieri and Prámparo, 2006; Zavala et al., 2024). Both palynofacies types have been interpreted as accumulated in periods of a relatively decreased water supply, and hence sediment influx to the basin. In the context of highly variable climatic conditions, the PT-B would represent the driest periods, and the PT-C could be pointed out as the transition between this condition and others much wetter, in which extraordinary precipitations could promote extraordinary fluvial discharges (PT-A). It is interesting to highlight that, in contrast with other lacustrine basins, such as the Cacheuta Basin (northwestern Mendoza, Argentina) in which the organic-rich shales (average TOC of 4 %, locally reaching 20 %) have a PM dominated by algal-derived organic matter (Zavattieri and Prámparo, 2006), the highest TOC percentages (MPEF-PALIN129 and MPEF-PALIN134 samples) are recorded in samples containing a kerogen of predominantly terrestrial origin (Tables 1 and S2), i.e. sporomorphs, phytoclasts, and fibrous AOM (Table 1, Fig. 9). This could be related to the relatively low initial H : C ratio (usually less than 1.0) and a high initial O : C ratio (up to 0.3; Tyson, 1995) in this type of organic matter. The preservation of this PM could be related to meromictic intervals in the lake. Tyson (1989) pointed out that during meromictic periods, highly organic-rich kerogenous shales are accumulated. The lack of mixing during these intervals could have favoured the intrinsic preservation potential of the organic matter in the basin. This could explain the two highest percentages registered in samples with a minimal autochthonous organic content (MPEF-PALIN129 and MPEF-PALIN134 samples). On the one hand, the complete predominance of terrestrial material in the PT-A, PT-C, and PT-D (Table S2, Fig. 9) mainly reflects a kerogen of Type III composition. On the other hand, the presence of strongly fluorescent organic matter including structured (i.e. *Botryococcus* colonies) and algal-derived amorphous material (i.e. spongy AOM, Table 1 organic categories) reaching up to 39.43 % of the total organic spectrum identified in the PT-B, suggest a mixed Type I/III kerogen composition.

The TAI values observed in the samples containing the palynomorphs selected for this analysis range from 2+ (PT-A1; Fig. 7d) to 3− (PT-C; Fig. 8a), indicating an early to middle-mature phase (oil/gas-prone; Pearson, 1990; Tyson, 1995). The fluorescence of the AOM and the sporomorphs is, in general, weak to moderate, with the exception of those recorded in the PT-B. Nevertheless, as the main proportion of the recovered PM is in accordance with the definition of kerogen Type III (sensu Tyson, 1995) – in terms of the nature of the organic matter, degree of preservation, and thermal maturity – these deposits appear to be a potential unconventional shale gas reservoir.

6 Conclusions

1. The Cañadón Asfalto Formation outcropping at the Cañadón Lahuincó locality documents a complete evolution of a lacustrine system, starting with an initial configuration and followed by a progressive basin infill. The integrated palynological, sedimentological, and sequence-stratigraphic analyses of the samples studied here enabled us to identify two depositional sequences, named Sequence I and Sequence II, controlled by different lake stages and depositional settings, as well as highly variable climatic conditions during the accumulation of these deposits. During Sequence I, the lake evolves from an underfilled to a balanced-fill/overfilled stage, while the beginning of Sequence II is marked by the return to underfilled conditions. Underlying these deposits, an overall coarsening-upward succession suggests the breaching of the lake spillpoint, marking the onset into overfilled lake conditions. These two opposite stages are bounded by a sharp contact, here interpreted as a forced-regression (FR) surface.

2. The recovered palynological matter is dominated by terrestrial-derived components showing a high organic allochthonous input to the basin. The relative variations between autochthonous (algae and algal-derived AOM) vs allochthonous (sporomorphs, phytoclasts, and terrestrial-derived AOM) palynological matter in the defined PTs suggest the alternation of relatively wetter and drier climatic periods during the accumulation of the underfilled, balanced-fill, and overfilled stages of the lake. Conversely, the samples studied in the upper overfilled succession (Sequence II) reflects the transition to more humid climatic conditions.

3. PT-A and PT-D would indicate the wetter periods, while PT-B suggests the development of relatively drier conditions. PT-C reflects the change among these two opposite situations. It is noteworthy the accumulation of alginite-rich structured organic matter (i.e. *Botryococcus* alga) during the drier intervals when the basin receives low volumes of water and clastic sediments. The

algal blooms provide the main material for the accumulation of Type I kerogen as well as the conditions to preserve the organic matter, depleting the oxygen of the bottom waters.

4. Two opposite taphonomic scenarios emerge from these deposits: on the one hand, the underfilled lake stage is characterised by low proportions and an overall poor preservation state of the terrestrial palynomorphs. On the other hand, the balanced-fill lake condition presents sporomorph-rich assemblages with relatively well-preserved spore and pollen grains, showing palaeoenvironmental conditions that favoured the preservation of the land-derived palynomorph's exine.

5. Palynofacies and TAI analyses suggest that the studied succession comprises early to middle-mature, gas-prone source rocks.

6. These results allow us to consider lacustrine basins as complex scenarios that are highly sensitive to palaeoenvironmental changes, such as climatic conditions. Differences in balance between precipitation and evaporation exert a high control on the nature, amount, and preservation degree of the organic matter accumulated in these deposits. Thus, refining the knowledge of the palaeoenvironmental evolution of lacustrine systems from different proxy data enables a more accurate understanding of the hydrocarbon source potential of this type of basin.

Appendix A: Alphabetical list of all identified species

Trilete spores
Deltoidospora australis (Couper) Pocock
Deltoidospora minor (Couper) Pocock
Dictyophyllidites harrisii Couper
Ischyosporites marburgensis de Jersey
Klukisporites lacunus Filatoff
Klukisporites spp.
Osmundacidites spp.
Retitriletes austroclavatidites (Cookson) Döring, Krutzsch, Mai, and Schulz in Krutzsch
Retitriletes semimuris (Danzé-Corsin and Laveine) McKellar
Verrucosisporites varians Volkheimer
Gymnosperm pollen grains
Alisporites lowoodensis de Jersey
Alisporites similis (Balme) Dettmann
Araucariacites australis Cookson ex Couper
Araucariacites fissus Reiser and Williams
Araucariacites pergranulatus Volkheimer
Araucariacites sp. cf. *A. pergranulatus* Volkheimer
*Araucariacite*s sp. A (Olivera, 2012, and bibliography therein)
Trilete spores
Callialasporites dampieri (Balme) Sukh Dev
Callialasporites microvelatus Schulz
Callialasporites segmentatus (Balme) Srivastava
Callialasporites trilobatus (Balme) Sukh Dev
Callialasporites turbatus (Balme) Schulz
Classopollis classoides (Pflug) Pocock and Jansonius
Classopollis intrareticulatus Volkheimer
Classopollis itunensis Pocock
Classopollis simplex (Danzé-Corsin and Laveine) Reiser and Williams
Classopollis torosus (Reissinger) Balme
Cerebropollenites macroverrucosus (Thiergart) Schulz
Inaperturopollenites indicus Srivastava
Inaperturopollenites giganteus Góczán
Inaperturopollenites microgranulatus Volkheimer
Inaperturopollenites cf. *reidi* (de Jersey) de Jersey
Inaperturopollenites sp. 1 (in Olivera, 2012)
Inaperturopollenites sp. 2 (in Olivera, 2012)
Indusiisporites parvisaccatus (de Jersey) de Jersey
Indusiisporites globosaccus (Filatoff) (in Olivera, 2012)
Indusiisporites sp. 2 (in Olivera, 2012)
Indusiisporites sp. 3 (in Olivera, 2012)
Microcachrydites antarcticus Cookson
Podocarpidites astrictus Haskel
Podocarpidites ellipticus (Cookson) Couper
Podocarpidites verrucosus Volkheimer
Podocarpidites sp. cf. *P. ellipticus* (Cookson) Couper
Podocarpidites sp. cf. *P. radiatus* Brenner
Podosporites variabilis Sukh Dev
Vitreisporites pallidus (Reissinger) Nilsson
Algae
Botryococcus sp. cf. *B. braunii* Kützing
Fungi
Annella capitata Srivastava

Code and data availability. The authors confirm that the data supporting the findings of this study are available in the article (Tables S1 and S2).

Supplement. Table S1. Quantitative distribution of major palynomorph groups in the Cañadón Asfalto Formation, Cañadón Lahuincó "A" section, expressed in percentages of total palynoflora based on a total count of at least 250 palynomorphs per sample. Table S2. Frequency distribution of the different recognised categories of PM based on the total count of 500 particles per sample. The supplement related to this article is available online at https://doi.org/10.5194/jm-45-335-2026-supplement.

Author contributions. DEO and CZ conducted the main conceptualisation. Formal analysis was carried out by DEO. DEO, CZ, and MQ conducted the investigation. DEO, CZ, and MQ carried out the methodology. The visualisation was prepared by DEO, CZ, and ES.

DEO and CZ prepared the paper (original draft preparation). Project administration was provided by CZ and RY. DEO, CZ, MQ, ES, RS, and RY did the critical review, commentary, and revision.

Competing interests. The contact author has declared that none of the authors has any competing interests.

Disclaimer. Publisher's note: Copernicus Publications remains neutral with regard to jurisdictional claims made in the text, published maps, institutional affiliations, or any other geographical representation in this paper. The authors bear the ultimate responsibility for providing appropriate place names. Views expressed in the text are those of the authors and do not necessarily reflect the views of the publisher.

Acknowledgements. The authors are grateful to Dres. Rubén Cúneo and Ignacio Escapa for field assistance and contributing resources during the fieldwork. The logistic support in the field provided by the Edigio Feruglio Museum and also the people who helped us with the fieldwork are greatly appreciated.

Financial support. This research has been supported by the National Natural Science Foundation of China (grant no. 42572178), the National Major Science and Technology Project of China (grant no. 2025ZD1400803), the Agencia Nacional de Promoción Científica y Tecnológica (grant no. PICT-2021-I-A-00871), and the Secretaría General de Ciencia y Tecnología, Universidad Nacional del Sur (grant no. PGI 24/H156).

Review statement. This paper was edited by Luke Mander and reviewed by Paula Narvaez and one anonymous referee.

References

Anderberg, M. R.: Cluster Analysis for Applications. Probability and Mathematical Statistics: A Series of Monographs and Textbooks, University Press Inc., New York, 359 pp., ISBN 978-0-12-057650-0, 1973.

Balme, B. E.: Fossil in situ spores and pollen grains: An annotated catalogue, Rev. Palaeobot. Palynol., 87, 1–323, https://doi.org/10.1016/0034-6667(95)93235-X, 1995.

Batten, D. J.: Identification of amorphous sedimentary organic matter by transmitted light microscopy, in: Petroleum Geochemistry and Exploration of Europe, Special Publications 12, edited by: Brooks, J., Geological Society of London, England, 275–287, https://doi.org/10.1144/GSL.SP.1983.012.01.28, 1983.

Batten, D. J.: Chapter 26A. Palynofacies and palaeoenvironmental interpretation, in: Palynology: Principles and Applications, edited by: Jansonius, J. and McGregor, D. C., AASP Foundation 3, 1011–1064, ISBN 9-931871-03-4, 1996.

Batten, D. J. and Morrison, L.: Methods of palynological preparation for palaeoenvironmental, source potential and organic maturation studies, in: Palynology-micropalaeontology: laboratories, equipment and methods, edited by: Costa, L. I., Bul. 2, Norwegian Petroleum Directorate, 35–53, 1983.

Behrensmeyer, A. K., Kidwell, S. M., and Gastaldo, R. A.: Taphonomy and paleobiology, Paleobiology, 26, 103–147, https://doi.org/10.1017/S0094837300026907, 2000.

Bohacs, K. M.: Relation of hydrocarbon reservoir potential to Lake-Basin type: An integrated approach to unraveling complex genetic relations among Fluvial, Lake-Plain, Lake Margin, and Lake Center Strata, in: Lacustrine sandstone reservoirs and hydrocarbon systems, edited by: Baganz, O. W., Bartov, Y., Bohacs, K. and Nummedal, D., AAPG Memoir, 95, 13–56, 2012.

Bohacs, K. M., Carroll, A. R., Neal, J. E., and Mankiewicz, P. J.: Lake-basin type, source potential, and hydrocarbon character: an integrated-sequence-stratigraphic–geochemical framework, in: Lake basins through space and time, edited by: Gierlowski-Kordesch, E. H and Kelts, K. R., AAPG Studies in Geology 46, 3–34, ISBN 0891810528, 2000.

Cabaleri, N. G. and Benavente, C. A.: Sedimentology and paleoenvironments of the Las Chacritas carbonate paleolake, Cañadón Asfalto Formation (Jurassic), Patagonia, Argentina, Sediment. Geol., 284–285, 91–105, https://doi.org/10.1016/j.sedgeo.2012.11.008, 2013.

Cabaleri, N., Armella, C., and Silva Nieto, D. G.: Saline lakes of Cañadón Asfalto (Middle Upper Jurassic), Cerro Cóndor, Chubut Province (Patagonia), Argentina, Facies, 51, 350–364, https://doi.org/10.1007/s10347-004-0042-5, 2005.

Cabaleri, N., Volkheimer, W., Armella, C., Gallego, O. F., Silva Nieto, D. G., Cagnoni, M. C., Ramos, A. M., Panarello, H. O., and Koukarski, M.: Estratigrafía, análisis de facies y paleoambientes de la Formación Cañadón Asfalto en el depocentro jurásico Cerro Cóndor, provincia del Chubut. Rev. Asoc. Geol. Argent., 66, 349–367, 2010.

Caccavari, M.: Dispersión del polen en *Araucaria angustifolia* (Bert.) O. Kuntze, Rev. Mus. Argent. Cs. Nat., 5, 135–138, 2003.

Carroll, A. R. and Bohacs, K. M.: Stratigraphic classification of ancient lakes: balancing tectonic and climatic control, Geology, 27, 99–102, https://doi.org/10.1130/0091-7613(1999)027<0099:SCOALB>2.3.CO;2, 1999.

Chalabe, A. C., Martinez, M. A., Olivera, D. E., Canale, N., and Ponce, J. J.: Palynological analysis of sandy hyperpycnal deposits of the Middle Jurassic, Lajas Formation, Neuquén Basin, Argentina, J. S. Am. Earth Sci., 116, 103867, https://doi.org/10.1016/j.jsames.2022.103867, 2022.

Chalabe, A. C., Olivera, D. E., Martínez, M. A., and Zavala, C.: Palaeoenvironments and palaeoclimate of the uppermost Cuyo Group and lowermost Lotena Group at Quebrada Álvarez, Picún Leufú Sub-basin, Patagonia, Argentina: a preliminary study based on palynology, Palynology, 48, 2254364, https://doi.org/10.5027/andgeoV52n2-3760, 2024.

Cúneo, R. N., Ramezani, J., Scasso, R. A., Pol, D., Escapa, I., Zavattieri, A. M., and Bowring, S. A.: High-precision U–Pb geochronology and a new chronostratigraphy for the Cañadón Asfalto Basin, Chubut, Central Patagonia: Implications for terrestrial faunal and floral evolution in Jurassic, Gondwana Res., 24, 1267–1275, https://doi.org/10.1016/j.gr.2013.01.010, 2013.

Cushing, E. J.: Redeposited pollen in Late Wisconsin pollen spectra from east-central Minnesota, Am. J. Sci., 262, 1075–1088, 1964.

De Jersey, N. J. and Raine, J. I.: Triassic and earliest Jurassic miospores from the Murihiku Supergroup, New Zealand, N. Z. Geol. Surv. Paleont. Bull., 62, 1–164, 1990.

Delcourt, P. A. and Delcourt, H. R.: Pollen preservation and Quaternary environmental history in the southeastern United States, Palynology, 4, 215–231, 1980.

Dettmann, M.: Upper Mesozoic microfloras from south-easterm Australia, P. Roy. Soc. Victoria, 77, 1–148, 1963.

Di Capua, A. and Scasso, R. A.: Sedimentological and petrographic evolution of a fluviolacustrine environment during the onset of volcanism: Volcanically-induced forcing of sedimentation and environmental responses, Sedimentology, 67, 1879–1913, https://doi.org/10.1111/sed.12681, 2020.

Falco, J. I., Hauser, N., Olivera, D. E., Bodnar, J., and Reimold, W. U.: A multi-proxy study of the Cerro Piche Graben-A Lower Jurassic basin in the central North Patagonian Massif, Argentina, J. S. Am. Earth Sci., 109, 103287, https://doi.org/10.1016/j.jsames.2021.103287, 2021.

Fantasia, A., Föllmi, K. B., Adatte, T., Spangenberg, J. E., Schoene, B., Barker, R. T., and Scasso, R. A.: Late Toarcian continental palaeoenvironmental conditions: An example from the Cañadón Asfalto Formation in southern Argentina, Gondwana Res., 89, 47–65, https://doi.org/10.1016/j.gr.2020.10.001, 2021.

Figari, E. G., Scasso, R., Cúneo, R. N., and Escapa, I.: Estratigrafía y evolución geológica de la Cuenca de Cañadón Asfalto, Provincia del Chubut, Arg. Lat. Am. J. Sedimentol. Basin Anal., 22, 135–169, 2015.

Filatoff, J.: Jurassic palynology of the Perth Basin, western Australia, Palaeontogr. Abt. B, 154, 1–113, 1975.

Fisher, J. S., Pickral, J., and Odum, W. E.: Organic detritus particles: initiation of motion criteria, Limnol. Oceanogr., 24, 529–32, 1979.

Grimm, E. C.: Tilia version 2.0.41 [software], Illinois State Museum, https://www.neotomadb.org/apps/tilia (last access: 8 May 2026), 2004.

Guy-Ohlson, D.: *Botryococcus* as an aid in the interpretation of palaeoenvironment and depositional processes, Rev. Palaeobot. Palyno., 71, 1–15, https://doi.org/10.1016/0034-6667(92)90155-A, 1992.

Hammer, D. A. T., Ryan, P. D., Hammer, Ø., and Harper, D. A. T.: Past: Paleontological Statistics Software Package for Education and Data Analysis, Palaeontol. Electron., 4, 178, http://palaeo-electronica.org/2001_1/past/issue1_01.htm, 2001.

Hart, G. F.: Maceral palynofacies of the Louisiana deltaic plain in terms of organic constituents and hydrocarbon potential, in: Sedimentation of organic particles, edited by: Traverse, A., Cambridge University Press, 141–176, ISBN 0 521 38436 2, 1994.

Holmes, P. L.: The soterring of spores and pollen by water: experimental and field evidences, in: Sedimentation of organic particles, edited by: Traverse, A., Cambridge University Press, 9–33, ISBN 0 521 38436 2, 1994.

Hutton, A. C., Kantsler, A. J., and Cook, A. C.: Organic matter in oil shales, Aust. Petrol. Explor. Ass. J., 20, 44–67, 1980.

Kovach, W. L.: Comparisons of multivariate analytical techniques for use in pre-Quaternary plant paleocology, Rev. Palaeobot. Palynol., 60, 255–282, https://doi.org/10.1016/0034-6667(89)90046-8, 1989.

Li, L. Q., Wang, Y. D., and Vajda, V.: Palynofacies analysis for interpreting paleoenvironment and hydrocarbon potential of Triassic–Jurassic strata in the Sichuan Basin, China, Palaeoworld, 30, 126–137, https://doi.org/10.1016/j.palwor.2020.04.007, 2021.

Lucas, F. A. and Omodolor, H. E.: Palynofacies analysis, organic thermal maturation and source rock evaluation of sedimentary succession from Oligocene to Early Miocene Age in X2 Well, Greater Ughelli Depobelt, Niger Delta Basin, Nigeria, J. Geosci. Geomat., 6, 85–93, 2018.

Maher, A.: *Classopollis* works as a significant indicator for the Cheirolepidiaceae paleovegetation arid zone, as proven by fossil records from Egypt, PLoS ONE, 20, e0318867, https://doi.org/10.1371/journal.pone.0318867, 2025.

Martínez, M. A., Olivera, D. E., Zavala, C., and Quattrocchio, M. E.: Palynotaphofacies analysis applied to Jurassic marine deposits, Neuquén Basin, Argentina, Facies, 62, 1–16, https://doi.org/10.1007/s10347-015-0457-1, 2016.

Martínez, M. A., Ferrer, N. C., and Asensio, M. A.: Primer registro de algas dulceacuícolas del Paleógeno de la Cuenca de Ñirihuau, Argentina: descripciones sistemáticas y análisis palinofacial, Ameghiniana, 45, 719–735, 2008a.

Martínez, M. A., Prámparo, M. B., Quattrocchio, M. E., and Zavala, C.: Depositional environments and hydrocarbon potential of the Middle Jurassic Los Molles Formation, Neuquén Basin, Argentina: palynofacies and organic geochemical data, Rev. Geol. Chile, 35, 279–305, https://doi.org/10.5027/andgeoV35n2-a05, 2008b.

McKellar, J. L.: Late Early to Late Jurassic palynology, biostratigraphy and palaeogeography of the Roma Shelf area, northwestern Surat Basin, Queensland, Australia (Including phytogeographic-palaeoclimatic implications of the *Callialasporites dampieri* and *Microcachryidites* Microfloras in the Jurassic–Early Cretaceous of Australia: an overview assessed against a background of floral change and true polar wander in the preceding late Palaeozoic-early Mesozoic) PhD thesis, University of Queensland, Australia, 469 pp., 1998.

Medeanic, S., Hirata, F., and Dillenburg, S. R.: Algal palynomorphs response to environmental changes in the Tramandai Lagoon, Southern Brazil, and climatic oscillations in the 20th century, J. Coast. Res., 26, 726–735, https://doi.org/10.2112/08-1175.1, 2010.

Mulder, T. and Syvitski, J. P.: Turbidity currents generated at river mouths during exceptional discharges to the world oceans, J. Geol., 103, 285–299, https://doi.org/10.1086/629747, 1995.

Mustafa, A. A. and Tyson, R.: Organic facies of Early Cretaceous synrift lacustrine source rocks from the Muglad Basin, Sudan, J. Petrol. Geol., 25, 351–366, https://doi.org/10.1111/j.1747-5457.2002.tb00013.x, 2002.

Nakayama, C.: Sedimentitas pre-Bayocianas en el extremo austral de la Sierra de Taquetrén, Chubut (Argentina), in: Proceeding of the 5th Congreso Geológico Argentino, Vol. 1, Villa Carlos Paz, 269–277, 1973.

Nip, M., Tegelaar, E. W., Brinkhuis, H., De Leeuw, J. W., Schenck, P. A., and Holloway, P. J.: Analysis of modern and fossil plant cuticles by Curie point Py-GC and Curie point Py-GC-MS: recognition of a new, highly aliphatic and resistant biopolymer, Org. Geochem., 10, 769–778, https://doi.org/10.1016/S0146-6380(86)80014-6, 1986.

Nullo, F. E. and Proserpio, C. A.: La Formación Taquetrén en Cañadón del Zaino (Chubut) y sus relaciones estratigráficas en

el ámbito de la Patagonia de acuerdo a la flora, Rev. Asoc. Geol. Argent., 30, 133–150, 1975.

Oboh-Ikuenobe, F. E. and de Villiers, S. E.: Dispersed organic matter in samples from the western continental shelf of Southern Africa: palynofacies assemblages and depositional environment of late Cretaceous and younger sediments, Palaeogeogr. Palaeocl. Palaeoecol., 201, 67–88, https://doi.org/10.1016/S0031-0182(03)00510-8, 2003.

Olivera, D. E.: Estudio palinológico y palinofacies del Jurásico Medio y Tardío de la Provincia de Chubut: Sistemática, Bioestratigrafía y Paleoecología, PhD thesis, Universidad Nacional del Sur, Argentina, 266 pp., https://repositoriodigital.uns.edu.ar/handle/123456789/503 (last access: 20 December 2025), 2012.

Olivera, D. E., Zavattieri, A. M., and Quattrocchio, M. E.: Palynology of the Cañadón Asfalto Formation (Jurassic), Cerro Cóndor depocenter, Cañadón Asfalto Basin, Patagonia, Argentina. Paleoecology and paleoclimate based on ecogroup analysis, Palynology, 39, 362–386, https://doi.org/10.1080/01916122.2014.988382, 2015.

Olivera, D. E., Martínez, M. A., Iturain, V. R., and Zavala, C.: New palynological insights into the Middle Jurassic Challacó Formation, Neuquén Basin, northwestern Patagonia, Argentina, Pap. Palaeontol., 11, e70011, https://doi.org/10.1002/spp2.70011, 2025.

Pankhurst, R. J., Leat, P. T., Sruoga, P., Rapela, C. W., Márquez, M., Storey, B. C., and Riley, T. R.: The Chon Aike province of Patagonia and related rocks in West Antarctica: a silicic large igneous province. J. Volcanol. Geoth. Res., 81, 113–136, https://doi.org/10.1016/S0377-0273(97)00070-X, 1998.

Papa, R. D., Wu, J. T., Baldia, S., Cho, C., Cruz, M. A., Saguiguit, A., and Aquino, R.: Blooms of the colonial green algae, *Botryococcus braunii* Kützing, in Paoay lake, Luzon island, Philippines, Philip. J. Syst. Biol., 2, 21–31, https://doi.org/10.3860/pjsb.v2i1.898, 2008.

Pearson, D. L.: Pollen/spore color "standard", version 2, Phillips Petroleum Company, Geology Branch, Oklahoma, p. 3, 1990.

Proserpio, C. A.: Descripción Geológica de la Hoja 44e, Valle General Racedo, Bol. de la Dirección Nac. de Min. y Geol., 201, 1–102, 1987.

Ravazzoli, I. A. and Sesana, F. L.: Descripción geológica de la Hoja 41c-Río Chico, Serv. Geol. Nacional Boletín, 148, 1–80, 1977.

Sajjadi, F. and Playford G.: Systematic and stratigraphic palynology of the Late Jurassic-earliest Cretaceous strata of the Eromanga Basin, Queesland, Australia: Part One, Palaeontogr. Abt. B, 261, 1–97, https://doi.org/10.1127/palb/261/2002/1, 2002.

Schwendemann, A. B., Wang, G., Mertz, M. L., Mcwilliams, R. T., Thatcher, S. L., and Osborn, J. M.: Aerodynamics of saccate pollen and its implications for wind pollination, Am. J. Bot. 94, 1371–1381, https://doi.org/10.3732/ajb.94.8.1371, 2007.

Silva Nieto, D., Cabaleri, N. G., Armella, C., Volkheimer, W., Gallego, O. F., Zavattieri, A. M., Giambiagi, L. B., Moschetti, M. A., and Mancuso, A.: Hipótesis sobre la evolución tectosedimentaria de los depocentros de la cuenca de Cañadón Asfalto (Jurásico–Cretácico), provincia del Chubut, Ameghiniana, 44, 67R, 2007.

Silva Nieto, D. G., Cabaleri, N., and Salani F.: Stratigraphy of the Cañadón Asfalto Formation, (Callovian-Oxfordian), Chubut province, Argentina, in: Proceeding of the 1st Simposio Argentino del Jurásico, La Plata, Argentina, Ameghiniana, 40, 46R, 2003.

Soreda, M. E.: Estudio sedimentológico y estratigráfico de la Formación Cañadón Asfalto en el área de Cerro Cóndor, Chubut, Argentina, Bachelor's thesis, Universidad Nacional de Buenos Aires, Ciudad Autónoma de Buenos Aires, Argentina, 136 pp., 2012.

Staplin, F. L.: Sedimentary organic matter, organic metamorphism, and oil and gas occurrence, B. Canad. Petrol. Geol., 17, 47–66, 1969.

Stipanicic, P., Rodrigo F., Baulíes O. L., and Martínez, C. G.: Las formaciones presenonianas en el dominio del Macizo Nordpatagónico y regiones adyacentes, Rev. Asoc. Geol. Argent., 23, 67–98, 1968.

Suarez-Ruiz, I., Flores, D., Mendonça Filho, J. G., and Hackley, P.: Review and update of the applications of organic petrology: Part 1, geological applications, Int. J. Coal Geol., 99, 54–112, https://doi.org/10.1016/j.coal.2012.02.004, 2012.

Tyson, R. V.: Late Jurassic palynofacies trends, Piper and Kimmeridge Clay Formations, UK onshore and offshore, in: Northwest European Micropalaeontology and Palynology, edited by: Batten, D. J. and Keen, M. C., Br. Micropal., Ellis Horwood Lmt., Chichester, England, 135–172, ISBN 0-7458-0498-5, 1989.

Tyson, R. V.: Sedimentary organic matter: Organic facies and palynofacies, Chapman and Hall, England, 615 pp., ISBN 978-94-010-4318-2, 1995.

Van Wagoner, J. C., Mitchum, R. M., Campion, K. M., and Rahmanian, V. D.: Siliciclastic sequence stratigraphy in well logs, cores, and outcrops, AAPG Meth. Explor. Ser., 7, 55, https://doi.org/10.1306/Mth7510, 1990.

Volkheimer, W.: Estratigrafía de la zona extrandina del departamento Cushamen (Chubut) entre los paralelos 42° y 42°30′ y los meridianos 70° y 71°, Rev. Asoc. Geol. Argent., 19, 85–107, 1964.

Volkheimer, W., Quattrocchio, M. E., Cabaleri, N., and García, V.: Palynology and paleoenvironment of the Jurassic lacustrine Cañadón Asfalto Formation at Cañadón Lahuincó locality, Chubut Province, Central Patagonia, Argentina, Rev. Esp. Micropaleontol., 40, 77–96, 2008.

Zavala, C., Liu, H. Q., Li, X. B., Trobbiani, V., Li, Y., Arcuri, M., and Zorzano, A. High-frequency lacustrine sequence stratigraphy of clastic lakes: lessons from ancient successions, J. Palaeogeogr., 13, 621–645, https://doi.org/10.1016/j.jop.2024.08.004, 2024.

Zavattieri, A. M. and Prámparo, M. B.: Freshwater algae from the Upper Triassic Cuyana Basin of Argentina: palaeoenvironmental implications, Palaeontology, 49, 1185–1209, https://doi.org/10.1111/j.1475-4983.2006.00596.x, 2006.

Zippi, P. A.: Freshwater algae from the Mattagami Formation (Albian), Ontario: paleoecology, botanical affinities, and systematic taxonomy, Micropaleontology, 44, 1–78, https://doi.org/10.2307/1485998, 1998.